Masters Program in Geospatial Technologies

SPATIOTEMPORAL ANALYSIS OF FOREST FIRE RISK MODELS: A CASE STUDY FOR A GREEK ISLAND

Stavros Sakellariou

Dissertation submitted in partial fulfilment of the requirements
for the Degree of *Master of Science in Geospatial Technologies*

NOVA IMS Information Management School
Universitat Jaume I
Westfälische Wilhelms-Universität Münster

SPATIOTEMPORAL ANALYSIS OF FOREST FIRE RISK MODELS: A CASE STUDY FOR A GREEK ISLAND

Dissertation supervised by

PhD Pedro da Costa Brito Cabral

Assistant Professor, Instituto Superior de Estatística e Gestão de Informação (ISEGI)

Universidade Nova de Lisboa (UNL), Lisbon, Portugal

Dissertation co-supervised by

PhD Mário Silvio Rochinha de Andrade Caetano

Associate Professor, Instituto Superior de Estatística e Gestão de Informação (ISEGI)

Universidade Nova de Lisboa (UNL), Lisbon, Portugal

Dissertation co-supervised by

PhD Filiberto Pla

Professor, Institute of New Imaging Technologies (INIT)

Universitat Jaume I (UJI), Castellón, Spain

February 2018

ACKNOWLEDGMENTS

Initially, I would like to thank the European Commission and the Consortium [1) Universidade Nova de Lisboa, NOVA - Information Management School, Lisboa, Portugal; 2) Westfälische Wilhelms-Universität Münster, Institute for Geoinformatics, Münster, Germany; 3) Universitat Jaume I, Castellón, Dept. Lenguajes y Sistemas Informaticos, Castellón, Spain] for awarding me the Erasmus Mundus scholarship.

I would like to express my gratitude to my supervisor *Pedro da Costa Brito Cabral* for his recommendations, corrections and the continuing guidance for the improvement and smooth completion of the thesis. In addition, I would like to thank my co-supervisors, namely, *Mário Silvio Rochinha de Andrade Caetano* and *Filiberto Pla*, for their valuable comments and suggestions and their contribution to my thesis.

In addition, many thanks to *Marco Octávio Trindade Painho* for the collaboration and his thoughtful suggestions during this Master program.

In the same context, I would like to thank all the staff of the Consortium and my fellows for this wonderful experience.

Furthermore, I would like to thank my daughter Ekaterini-Barbara; my wife Paraskevi; my parents, Panagiotis and Ekaterini; my brother Spyridon; my sister Vasiliki; father Ioannis and all my relatives and friends from Greece for their continuing support.

Most importantly, I am too grateful to *Jesus Christ* who supported me with any means all these years to successfully complete the thesis and the entire Master program.

SPATIOTEMPORAL ANALYSIS OF FOREST FIRE RISK MODELS: A CASE STUDY FOR A GREEK ISLAND

ABSTRACT

Forest fires are a natural phenomenon which might have severe implications on natural and anthropogenic ecosystems. Consequently, the integrated protection of these ecosystems from forest fires is of high priority. The aim of the project lies in the development of two preventive models which will act in synergy in order to effectively protect the most critical natural resource of the island, namely, the abundant forests. Thus, fire risk modeling is combined with visibility analysis, so that we may primarily protect the most susceptible territory of the study area. The corner stone of the methodology is primarily relied on the multi-criteria decision analysis. This framework applied not only for the fire risk estimation and the corresponding evolution in a context of 20 years, but for visibility analysis as well, determining the most suitable locations for the establishment of a minimum number of watchtowers. The fire risk map for 2016 indicated that 34% of the entire study area is covered by territory of low fire risk; 27% of moderate risk; 34% of high and very high risk, while there is a 6% of the island which is characterized by extremely fire risk. Similar conclusions can be drawn for 1996, since no significant changes have been observed, especially on the land cover types and their spatial arrangement. Based on the visibility results, more than 40% of the entire island is visible from the selected location scheme consisting of just 8 watchtowers. The intense topography constituted the most critical barrier in increasing this percentage. Some good practices to counterbalance the relative small percentage of visibility could include; the extensive patrols in unmonitored regions through the intense road network of the island; the adoption of drones covering the aforementioned areas, especially when extreme meteorological conditions are expected.

KEYWORDS

Forest fires

Multi criteria analysis

Fire risk

Spatiotemporal analysis

Visibility

Geographical Information Systems

Remote Sensing

Skiathos island

Greece

ACRONYMS

AHP – Analytic Hierarchy Process

AUC – Area Under Curve

CLC – Corine Land Cover

DEM – Digital Elevation Model

DRGI – Dynamic Relative Greenness Index

GIS – Geographical Information Systems

GPS – Global Positioning System

IRS – Indian Remote Sensing

MCDA – Multi-Criteria Decision Analysis

MODIS – Moderate Resolution Imaging Spectroradiometer

NDVI – Normalized Difference Vegetation Index

NDMI – Normalized Difference Moisture Index

NIR – Near Infrared

NOOA – National Oceanic and Atmospheric Administration

SWIR – Shortwave Infrared

INDEX OF THE TEXT

INDEX OF TABLES

INDEX OF FIGURES

1. INTRODUCTION

1.1 Motivation and rationale

Forest fires are a natural phenomenon which might have severe implications on natural and anthropogenic ecosystems. The Mediterranean countries face such events almost every year. Indicatively, representative fire statistics highlight the significance of the phenomenon in one of them, namely, in Greece. For instance, 1.613 forest fires incidents have been recorded in Greece burning 29,144 ha of forest lands in just one year (2011). Cumulatively, in a timeframe of fifteen years (1983-2008), 1.361.312 ha of forest area has been affected by fires. The annual values reached 1.465 fire hotspots, leading to 52.358 ha of burned area (Tsagari et al. 2011). Translating the impacts of one of the most damaging fire incidents in the history of Greece in 2007 to quantitative terms, we observed that more than half a million people were affected, while the financial cost of these damages reached approximately three billion Euro (Mitsakis et al. 2014).

Islands can be considered quite susceptible environments where any critical change may drastically affect every perspective of this territory, from the natural and cultural environment to socioeconomic life and cohesion. The island of Skiathos in Greece constitutes a unique case due to the fact that it is a highly touristic island and preserves forests and landscapes of extraordinary beauty. Hence, this natural asset must be preserved and protected from one of the most damaging factors, namely, forest fires. Focusing on the main point of fires effects, Sakellariou et al. (2017) cited "*destructive and recurrent forest fires (of high intensity) are one of the greatest hazards for the viability and sustainable development of forests, and have impacts on natural and cultural environments, and the economy and the quality of life of local and regional populations*".

Consequently, the integrated protection of the island from natural and anthropogenic factors which might heavily degrade the natural resources of the study area is of high priority. Due to the general difficulty to suppress effectively a destructive forest fire, special attention will be given to the prevention of such complicated phenomena, before they take enormous dimensions with unpredictable implications (loss of human lives; degradation of natural ecosystems; increased levels of erosion which may lead to flood events; economic loss from tangible and intangible forest products etc.).

1.2 Aim and specific objectives

The aim of the project lies in the development of two preventive models which will act in synergy in order to effectively protect the most critical natural resource of the island, namely, the abundant forests. Thus, fire risk modeling (based on the impact of natural and anthropogenic factors to fire risk) is combined with visibility analysis, so that we may primarily protect the most susceptible territory of the study area.

Specific objectives will support the implementation of fire risk modeling and visibility analysis. Specifically, these objectives consist of:

- The exploration of individual natural and anthropogenic key factors that may heavily affect the fire risk. More specifically, the exploration of vegetation characteristics to the possible fire behavior (type of forest fuels); the determination of vegetation conditions and ground humidity through estimating the Normalized Difference Vegetation Index (NDVI) and the Normalized Difference Moisture Index respectively; the effect of topography, such as the elevation, slope and aspect, as estimated by the Digital Elevation Model (DEM); and the scalable influence of roads and towns proximity to forests (where most fire incidents take place).
- The determination of fire risk for two reference years (1996 and 2016) through multi-criteria analysis in order to detect both the most vulnerable regions of the island and the potential spatiotemporal changes that could be resulted from the distinct effect of any critical factor. This fact will allow us to focus on specific prevention measures based on the influence of each contributing factor.
- Final objective constitutes the establishment of optimal locations of watchtowers through visibility analysis. This analysis focuses on the covering of the most vulnerable areas (based on the fire risk map) for immediate detection and suppression of fire events.

Hence, the project is based on two distinct but interrelated pillars. Firstly, multi-criteria analysis takes place exploring the collective contribution of the key factors to fire risk. The final determination of fire risk is a knowledge-based approach integrating the variable influence of each natural and anthropogenic factor, such as: topography, land cover, vegetation indices, proximity to road and human settlements network. This process has been repeated for two reference years (1996, 2016) in order to determine the spatiotemporal evolution of fire risk and the potential causes that may lead to these changes. Afterwards, visibility analysis was combined with the fire risk modeling. Consequently, a second process of multi-criteria analysis was conducted in conjunction with viewshed analysis in order to determine the most appropriate locations for the establishment of watchtowers in terms of surface appropriateness (most susceptible areas, relatively high elevation, avoiding water surfaces etc.) and visibility potential. Thus, a synergistic prevention effect may increase the possibilities of early fire detection, especially on the most vulnerable territories.

2. THEORETICAL FRAMEWORK

Fire risk modeling itself constitutes a complex and multifaceted process since natural phenomena are characterized by a high degree of uncertainties. However, the inter-annual cumulative knowledge for the management of forest fires has allowed us to determine some specific aspects in order to deal with this phenomenon as efficiently as possible. To this end, sophisticated technologies have been a powerful tool in assisting rational and effective decision making. Hence, the interplay of key factors have been analyzed with the aid of GIS and remote sensing so that we can estimate the most vulnerable areas and apply appropriate measures such as the establishment of watchtowers. Thus, this chapter explores the GIS-based multi criteria analysis in a broad range of fields, followed by the specification of this methodology to fire risk. Finally, visibility analysis is described, applied to diverse fields, while a few studies focus on forest fires phenomenon.

2.1 GIS-based multi criteria decision analysis

There are many applications in the literature that use specific GIS and other multicriteria decision analysis (MCDA) techniques either for evaluation of land suitability for different reasons (fire risk, landslide vulnerability, land use planning) or for the finding of optimal locations based on the desired purpose (wind farm or industrial units locations).

Van Haaren and Fthenakis (2011) explored the optimal location of a wind farm, based on a specific number of criteria. Those criteria were related to economic (cost related to the acquirement of the supporting land and the road construction); planning (related to visual effect and noise pollution, interference with other critical land uses, e.g. airport etc.); topographical (slope) and ecological (proximity to birds' habitat etc.) factors. In the same context, Villacreses et al. (2017) and Noorollahi et al. (2016) explored the most appropriate location for establishing a wind farm, relied on many interacting factors such as: wind characteristics; land surface suitability and proximity to road network and other crucial infrastructure.

Chen et al. (2010) implemented suitability analysis for irrigation purposes, relied on the interaction of some certain criteria (hydraulic properties of soil, slope, soil types, etc.). Emphasis was given on the importance of the weighting process and its impact (through sensitivity analysis) on the final results. Yalcin and Gul (2017) took advantage of GIS multi criteria decision framework along with Analytical Hierarchy Process (AHP) in order to discover new potential geothermal hotspots (indicative criteria: closeness to hot springs, extreme differences on land surface temperature etc.).

Hariz et al. (2017) explored the optimal location for a healthcare waste incinerator based on a range of factors. Specifically, they took into consideration economic (e.g. road and electric network accessibility), social (e.g. interaction of urban and rural regions) and environmental criteria (e.g. land use and soil type and characteristics). Hence, they integrated all the above dimensions into a GIS framework in conjunction with other multicriteria analysis techniques (e.g. AHP etc.).

On the other hand, Erener et al. (2012) examined the landside vulnerability through a series of cartographic products derived from the comparative assessment of three multicriteria methods, namely, *GIS-based multi-criteria decision analysis, logistic regression, and association rule mining*. Some of the most contributing factors to landslide susceptibility that were included in the above models are: land use and soil types characteristics, topography, proximity to infrastructure, faults etc.

Sánchez-Lozano and Bernal-Conesa (2017) proceeded to effective environmental management of some critical natural regions that belonged to military agency. To this end, they used GIS and other multicriteria decision analysis techniques in order to achieve the best possible results. The effective environmental management may involve specific actions like forest fire protection, rehabilitation of areas suffered from any artificial process, official recording and protection of flora and fauna species, drastically dealing with regions suffered from severe pollution etc. In order to accomplish all the aforementioned objectives, they defined specific criteria such as: proximity to human settlements, road network and agricultural fields; topography (slope); proximity to ecological corridors; proximity to areas subject to severe pollution; desertification hazard etc. Finally, they used two techniques, namely *AHP* and *Technique for Order of Preference by Similarity to Ideal Solution* for the final ranking of the involved parameters. The combination of GIS and the other two MCDA techniques provided the hierarchy of areas that are considered of utmost importance for efficient and urgent environmental management.

In addition, Zhang et al. (2012) tried to implement a GIS multicriteria decision framework in order to better manage and solve the contradicting forces in land use planning between different types of land uses and the involved stakeholders.

Finally, such a GIS-based MCDA framework is widely used for finding the best location for industrial units. Rikalovic et al. (2014) implemented that model in order to determine the optimal location of an industrial facility taking into account all the vital economic factors related to this kind of problem. Some of these criteria (either as favorable or limiting factors) included the proximity to road network, the proximity to protected areas; and proximity to water bodies. Definitely, other substantial factors could be included in this model, for instance, monetary value of land, topographic characteristics etc. The integration of all these parameters yielded the best location for this specific industrial unit.

Based on the above projects, it should be highlighted the high added value of GIS applied to a totally diverse domains (energy; environmental management; industry etc.), focusing on the interrelation of key factors and finding the most appropriate locations relied on specific objectives as determined in each scientific field. In the next section, the evaluation of forest fires risk modeling under a multicriteria decision framework is discussed in depth through the literature review of projects of similar nature.

2.2 Fire risk analysis

A significant aspect of the interplay between GIS and forest fires prevention constitutes the establishment of fire risk maps relied on the local characteristics of the study area.

In this context, Eugenio et al. (2016) estimated the fire risk of a study region in Brazil, not only based on the surface characteristics of the area, but also exploring another contributing factor; namely climatological features. In brief, the model included: i) the exploration of the precipitation influence, mapping this feature relied on the exponential kriging technique; ii) the potential evapotranspiration, water deficit and mean temperature influence, mapping those features based on the spherical kriging technique; iii) the influence of the surface factors such as elevation, slope and aspect derived from the Digital Elevation Model; and the contribution of land uses and road network (due to proximity to forested areas) to forest fires ignition. Finally, applying AHP techniques, specific weights were assigned for each and every variable. Map Algebra tool (integrated into GIS) combined all the above information, so that the final risk map to be created.

Sivrikaya et al. (2014) explored the fire risk potential based on the natural and anthropogenic dimensions. These inputs included: i) the influence of forest features such as the vegetation/fuel types, the crown closure as well as the age characteristics of the species; ii) the effect of geomorphology, such as the slope and aspect of the study area. Both characteristics may intensely contribute to fire propagation, and iii) the influence of human factor (socioeconomic activities; accidents etc.) which can be found on anthropogenic structures, such as the human settlements and the road network. Around these conceivable zones, the majority of fire ignitions take place. The interaction of all the aforementioned factors lead to a united fire risk map taking into advantage the analytical capabilities of GIS.

Amalina et al. (2016) developed a similar susceptibility map combining data and tools of remote sensing and GIS. Specifically, they created several thematic maps, each one representing the contribution of each variable to forest fire ignition and behavior. So, they combined: i) the land uses layer derived from satellite images after the classification through Maximum Likelihood algorithm; ii) vegetation and climatological indices such as the Normalized Difference Vegetation Index (NDVI), the Normalized Difference Moisture Index (NDMI) and the estimation of surface temperature along the study domain (exploiting the remote sensing techniques); iii) and the scalable distance from certain anthropogenic (towns, roads etc.) and natural structures (water surfaces; specific crop cultivations etc.). Next, they evaluated each factor based on their impact to forest fires phenomenon, assigning them with a distinct weight. Finally, they constructed an equation integrating all these factors. The final output was the fire risk map. Here, it should be noted that they assessed the natural and anthropogenic factors interchangeably as a dominant player to forest fires each time (10% vs 90% of contribution). However, there is no any concrete argument to provide a 90% weight to human factor and that is why, they rejected this hypothesis in the end.

Kant Sharma et al. (2012) used a similar multicriteria decision analysis framework in order to create the fire risk map. They combined remote sensing and GIS data and techniques, such as forest types characteristics, topography (elevation, slope and aspect) and the proximity zones to human structures. Finally, they integrated all these variables under three distinct techniques, namely, *the knowledge-based, the crisp and fuzzy analytical hierarchy process (AHP)* in order to cope with the uncertainties inherent into forest fires phenomenon. It should be noted that the last two methods (AHP) provided almost identical results and they were characterized with a certain degree of difference in relation to the first technique.

A comprehensive web-based decision support system for fire prevention exploiting remote sensing and GIS data and methods, was implemented by Roberto Barbosa et al. (2010). First of all, the majority of the data was derived from satellite sources, such as the acquirement of active fire hotspots file; the meteorological data and the corresponding images which were used for land use classification and the development of the Digital Elevation Model. The file with the active hotspots could be depicted immediately with the appropriate process of geocoding. At the same time, spatial interpolation techniques took place for the creation of the respective meteorological thematic maps. Following, they performed supervised classification of the satellite image in order to generate the thematic map of land uses. After that, they reclassified all the involved variables based on their contribution to forest fires ignition and propagation. These factors included: the maximum and minimum temperature; the level of precipitation; the unified layer of wind characteristics (velocity and direction) along with one element of topography (aspect) given that the vector of these three variables may have a significant impact (cumulatively); the maximum and minimum relative humidity; the land use and the slope layers. All the aforementioned factors were evaluated and ranked (knowledge-based) according to their distinct impact to forest fires. Finally, a specific equation integrated all these dimensions, giving an additional external weight to the general contribution of each factor to the under-study phenomenon. Hence, the magnitude of any hotspot could be estimated based on the location on the fire risk map. This process may prioritize and allocate the respective firefighting forces to different events based on the magnitude of the fire.

Vadrevu et al. (2010) developed a fire risk map using multi criteria decision analysis combining the AHP and the Fuzzy Set theory integrated into a GIS environment. Specifically, they created a structure of two kinds of criteria. One more general which included: the geomorphology; the vegetation characteristics; the climatic and socioeconomic/demographic variables. Under these categories, more specific criteria were adopted such as: Geomorphology: elevation, slope, aspect and a composite topographic index related to ground moisture; Vegetation characteristics: dry deciduous species, biomass density and an index which is related to the amount of energy released when the wood is burned; Climatic variables: mean temperature and rainfall in the hottest season and the amount of evapotranspiration; Socioeconomic/demographic variables: population density, literacy rate, number of staff employed on the primary sector of economy (especially agriculture) and nutritional density. All these specific variables were assigned distinct weights based on the fuzzy set

theory techniques, while the first level (more general categories) were subjected to AHP technique. Finally, these frameworks were integrated into a GIS environment and through map algebra, the final risk map was created. Here, it should be stressed that for some of these variables (especially the socioeconomic ones, e.g. nutritional density etc.), there is no any concrete theoretical background that explains with safety their inclusion (contribution) to the development of the fire risk map.

You et al. (2017) evaluated the forest fire risk in a world heritage site and proceeded to the spatiotemporal analysis of risk in a timeframe of twelve years. They integrated geomorphological (slope, aspect and elevation through the DEM) and meteorological factors (temperature, level of rainfall and evapotranspiration); vegetation features (fuels types and humidity, development stage and canopy density) and human structures (closeness to towns, agricultural roads, water bodies and land uses). They assessed the special weight of all these variables based on AHP technique and developed the final risk map through map algebra which is an inherent component of GIS. Finally, the applied spatial statistics techniques (Exploratory Spatial Data Analysis, Spatial autocorrelation indices etc.) in order to reveal specific spatial patterns (e.g. different types of clustering) of fire risk evolving through the time.

Pradhan et al. (2007) created a susceptibility map based on the interrelation of fire events and the respective contributing factor. So, they collected the fire hot spots from NOAA satellites for five consecutive years. Afterwards, they classified the satellite image through unsupervised classification in order to form the land use map. At the same time, they calculated the NDVI and used other meteorological and topographic inputs such as soil features, slope, and aspect. Finally, they assessed the impact of each and every factor in relation to the fire hotspots. Based on this *frequency ratio* technique, they estimated the corresponding weights for all the variables and developed the final risk map.

Saglam et al. (2008) explored two forest fires interrelated indices, namely, forest fire risk and forest fire danger and proceeded to the spatiotemporal analysis from 1987 to 2000 with emphasis on forest fuels characteristics. Firstly, they created the forest types maps with the contribution of Landsat imagery, and ground truth information providing details about specific features of fuels. Thus, they implemented the supervised classification based on maximum likelihood algorithm. Next, they discriminated the terms of fire risk and danger, where the former indicates the "*probability of ignition*" based on the contributing factors, while the latter "*refers to sum of constant and variable factors affecting the ignition, spread, and resistance to control, and subsequent fire damage*". Afterwards, for the first index, they estimated the contributing impact of fuel types, topography (slope and aspect) and the closeness to human structures and infrastructures where most activities take place (agricultural fields, inhabited areas). On the other hand, the fire danger index included the effect of vegetation characteristics (fuel types, age stage of species, crown closure) and topography. Even though they proceeded to knowledge based evaluation of the variables in relation to fire risk, different equations described the meaning of the above terms. Finally, they studied the spatiotemporal analysis

of fire risk solely relied on the specific forest fuels features, without taking into account the other factors. Definitely, vegetation characteristics is the key factor on fire risk determination, however, other variables have their added value to the composition of such indices.

Kalabokidis et al. (2013) developed an online application taking the advantage of GIS tools and methods as well as the acquirement and process of other geospatial information (satellite images; meteorological data etc.) for interactively manipulating forest fires in real time. The application consisted of several modules. The first one was related with the active management of forest fires using certain inputs and processes such as: satellite and aerial maps; thematic maps of elevation, road network, land cover, evacuation regions, fire observatories, and other human structures and infrastructure; a similar to geocoding process to locate firefighting vehicles and airtankers which are equipped with GPS trackers; real time valuable geoprocessing options (estimation of the optimal route to the nearest water tank etc.); The second module incorporated the design of the appropriate meteorological (thematic) maps (temperature; relative humidity; rainfall, wind features etc.). These maps represent the variables that are conducive to forest fires phenomena; the third module was responsible for the determination of fire risk through the *Fire Ignition Index*. This index integrated the key factors that may trigger and propagate forest fires phenomena. Specifically, it combined four sub-indices, namely, the *Fire Weather Index* (temperature, wind speed, level of rainfall and relative humidity); the *Fire Hazard Index* (fuels characteristics and topographic variables) and the *Fire Risk Index* (proximity to road network, inhabited areas, agricultural fields, and other infrastructure such as power lines). Finally, the application incorporated a fire propagation model for simulating forest fires phenomena based on the American *FARSITE* fire simulation model which is fed from the aforementioned inputs.

Carmel et al. (2009) estimated the fire risk of a mountainous region using a fire simulation model, namely, the American *FARSITE*. After a significant number of simulations, the fire risk was determined based on the results of this model such as the ignition and the burned area resulted from the simulations. Key variables were included in the model with the most significant one to be the fuel types, while a sub-model would determine the fire behavior per vegetation species. Other critical factors incorporated in the model were: topography; fuel characteristics (moisture and crown closure etc.); meteorological factors (wind velocity and direction, relative humidity, temperature); the location of ignition point which was a random process. However, the authors estimated that most fire events occur in proximity to road network. So, they created distinct buffer zones per type of road network and the majority of the random ignition points (approximately 80%) fell into these zones. The remaining 20% of the hotspots broke out in other places of the study domain; and the timeframe of burning was adjusted based on historical data (past records). Finally, based on all these simulations, a fire risk map was created and it was similar to the spatial structure of fuels. Nevertheless, the other critical factors (topography etc.) played their important role modifying the fire risk in many neighboring areas despite the existence of the same fuel types.

Gai et al. (2011) developed a forest fire risk based on the three interrelated factors. The first one is related to the physical features of the study area, the second is associated with socioeconomic variables and the last one is linked to the accessibility of the fire fighting forces and infrastructure. Specifically, they integrated: topography (elevation, slope and aspect), land use and meteorological information (temperature, moisture and wind speed); population density and worth of forested areas; and the proximity from fire agency premises, fire observatories and firefighting helicopter location. Beyond the distinct weighting of all these factors, they determined an external weight for each variable based on *Grey Relativity Analysis*. Finally, after they created the fire risk maps for each general category, they developed the united fire risk map integrating all the above key factors. However, it should be noted that *Grey Relativity Analysis* provided general weights that were almost identical for all factors (with slight differences), a fact that might be not true, especially when compared the impact of fuels with other less minor factor (such as elevation, or worth of forested area). In the same context, it should be highlighted that the distance from fire observatories might play absolutely no role in fire risk determination, but it might have crucial role in early detection of fire events which is of crucial importance.

One of the initial forest fires risk maps was implemented by Jaiswal et al. (2002). The authors created a forest types map through classification of remotely sensed data derived from IRS 1D satellite. Afterwards, they chose to explore and map other crucial factors, namely, slope, and proximity to human structures and infrastructure (towns and road network). After the weighting process to each variable and to the general category to which those variables belonged, they integrated all these inputs in order to create the final risk map. However, other vital factors were absent. In the following years, several additional contributing factors have enriched those fire risk models.

Gabban et al. (2006) estimated the fire risk for the Mediterranean countries relied on exclusively remotely sensed data. Specifically, they created this index based on the temporal evolution of NDVI values, derived from *NOAA - Advanced Very High Resolution Radiometer* data. The authors emphasized that the determination of fire risk based on NDVI index could effectively be calculated through a temporal evolution of this index. To this end, they created an index called *Dynamic Relative Greenness Index (DRGI)*, which combined the NDVI value of each pixel in relation to the corresponding minimum and maximum NDVI values (retrieved by past records on daily basis). After the validation of this model, they concluded that there is a high correlation between this index and the number of fire events. Thus, the lower the DRGI the more possibilities to have greater number of fire hotspots.

Pourghasemi (2016) enriched the fire risk map with additional variables on the one hand, and on the other hand, he proceeded to a comparative analysis of two statistical methods for determining the specific weights per involved variable. The model incorporated the following key factors: topography (slope, aspect and elevation); topographic position and wetness indices (indices related to elevation and slope); plan curvature (all the above indices were being extracted from the DEM of the study

area); proximity to natural and anthropogenic elements (water bodies, inhabited areas and road network); land use; NDVI; soil types; and meteorological variables (rainfall, temperature and wind features). At the same time, he used 70% of the (historical) fire hotspots as a training dataset and 30% for validation purposes. This data was retrieved from MODIS platform and will be used for the validation of the following models. Next, he applied the *evidential belief function* in order to determine the special weight of each sub-class inside all variables in relation to the number of hot spots per sub class. Finally, they combined all the aforementioned factors, after the multiplication of each sub class with the respective weight, and created the first fire risk map. The second approach included the determination of the weights based on the *binary logistic regression*. After the comparison of the two methods based on the estimation of the *area under curve* (AUC), he concluded that the logistic regression approach was performed better than the evidential belief. Even though it might be a robust method, it should be highlighted the fact that some correction measures should have been taken based on the literature review and general knowledge of the phenomenon. One example consists of the high weight (evidential belief) on very high levels of elevation, where beyond a natural cause (e.g. a thunder), the possibility of a fire ignition is considered low due to multiple interrelated factors (distant from anthropogenic structures; high levels of ground moisture and lower temperatures).

Concluding, it should be stressed that fire risk modeling is estimated by different tools and methodologies aiming to achieving the most reliable results. The primary inputs are quite similar providing the framework for a detailed analysis of fire risk. GIS, AHP, Fuzzy logic, statistical techniques and remote sensing indices are widely used for the improvement of final result with very successful results.

However, in order to establish the validity and superiority of each method over the others, a comparative assessment of different methods in any study area with the same inputs could be a first indication of the robustness of different techniques, as it happens when comparing different classification algorithms in remote sensing. Definitely, beyond the same inputs, we should use the same validation method and data in order to compare the effectiveness of these techniques. In addition, it should be noted that there are very few studies exploring the spatiotemporal evolution of fire risk determining the capacity of each contributing factor to fire risk through time and suggesting the most appropriate measures.

2.3 Visibility analysis

Viewshed analysis has been used in many scientific and practical applications. The main purpose of this analysis can be considered multifaceted based on the specific objective of each project. Following, several examples are presented, so that we can formulate an idea about the added value of this tool.

Mouflis et al. (2008) explored the temporal visual pollution of marble quarry growth through time in a Greek island. This process (if not managed effectively) may have a severe impact on other crucial socioeconomic activities such as tourism, reducing attractiveness of the natural environment of the island.

Rød and van der Meer (2009) studied the visual influence of a significant proposed project which included the construction of a very tall building in the downtown. After they have implemented a viewshed analysis, the authors concluded that the new structure would not have severe visual effect from specific locations as determined by the local planning authorities.

Other applications include the visual effect analysis on natural environment, derived from certain economic activities of the primary sector of economy such as the mining industry (Zhou et al. 2011). Falconer et al. (2013) used the viewshed analysis in order to find an optimal location (with the least visual effect) for aquaculture activities, while Castro et al. (2011) exploited this tool to promote safety in the transportation sector (e.g. visible distance on motorways). Wróżyński et al. (2016) explored and studied the visual intrusion of wind generators, a key factor that definitely affects the final location of such investments. To this end, they combined visibility analysis and 3D models for more reliable results.

Visibility or viewshed analysis is a powerful tool in order to determine the visual pollution or intrusion of certain structures or economic activities. So, public acceptance can be guaranteed reducing or appropriately managing the visual impacts of any new investment.

2.3.1 Visibility analysis in forest fires

Pompa-García et al. (2010, 2012) designed a simple visibility model for early detection of forest fires. The primary data used were the Digital Elevation Model (DEM) of the study area and the corresponding land cover / forest types. Even though, these specific models could have their own added value covering most of the vulnerable forest fuels, there was no any concrete methodology or reasoning (except the aim of the project which was the maximum visibility coverage from the least possible observers) for selecting the specific locations of watchtowers.

A most integrated approach of visibility analysis in forest fires prevention is presented by Eugenio et al. (2016b). More concisely, they developed a coherent model taking into consideration multiple factors such as: i) the elevation and the geomorphology of the study area through the DEM; ii) the selection of the most appropriate land uses in terms of human resources accessibility and appropriate surface for locating the watchtowers, avoiding rocky, water or other inappropriate surfaces; iii) following, they created multiple ring buffers (100; 300; and 500 meters) along the road network, so that they may assure the proximity of roads and the towers (small walking distance); iv) next, they applied *stratified unaligned systematic sampling* for the creation of point database as potential positions of the proposed watchtowers; v) after the intersection of multiple ring buffers and their other respective characteristics as described above, they created grids with distinct dimensions (15x15 km;

17.5x17.5 km; 20x20 km) selecting all the highest positions within each division; vi) finally, the locations with higher altitudes were selected for each method and visibility analysis applied for all these candidate positions. Last, in order to examine the validity of their model, they overlaid the proposed method, in terms of visible area, with the areas of high - very high risk and conservation units as well as with the area where the most fire hot spots have outburst.

In the same context, Bao et al. (2015) explored the optimal locations of watchtowers for early detection of forest fires. The primary data used were a certain number of potential locations on the ridge and the DEM of the study domain. Subsequently, they combined spatial optimization techniques and viewshed analysis. Specifically, they implemented three models relied on basic assumptions such as: i) the coverage of the entire study area in terms of visibility in conjunction with the least cost of construction; ii) achieving maximum visible area coupled with the least cost of construction; and iii) accomplishing maximum visible area based on specific amount of funding for the construction of the watchtowers. For the implementation of all these objectives, they used programming techniques and genetic algorithms, concluding that after a certain percentage of visibility (after the optimization processes), the marginal added value of additional watchtowers is getting quite small in a cost-benefit analysis.

Concluding, it should be emphasized that visibility or viewshed analysis and applications for forest fires prevention are quite limited. So, there is fertile ground to apply this technique of high added value to forest fires field in order to detect any incident as soon as possible minimizing the extensive consequences of uncontrollable phenomena. The adoption of programming and optimization techniques (i.e. genetic algorithms) could improve the final result in terms of visibility effectiveness, reducing significantly the computation time.

Finally, it should be mentioned that even though fire risk modeling and viewshed analysis consist of two interrelated fire prevention measures, there are very few studies focusing on this interaction. Hence, the current study tries to bridge this research gap, not only exploring the spatiotemporal analysis of fire risk, but also putting the fire risk and viewshed analysis into the same framework maximizing the efficiency of forest fires prevention.

3. Materials and Methods

This chapter presents the exact geographic location of the study area as well as the primary inputs that will be used in fire risk modeling for the reference years. Some essential pre-processing techniques have been conducted so that we can use these factors directly into the fire risk framework. The primary inputs consist of topography (elevation, slope, aspect); land cover; vegetation indices (NDVI, NDMI); proximity to road and human settlements network. The analysis of these inputs leads to the justification of adopting the specific fire risk model.

3.1 Geographical location

The study area of the project constitutes a small Greek island, which is called Skiathos. The island of Skiathos is situated in the central area of Greece and belongs to the Prefecture of Sporades (Figure 3.1). The geographic coordinates of the study area are: 39°10′N 23°29′E (Wikipedia, 2017).

The population of the island remained almost stable in a timeframe of the last ten years. Specifically, a tiny population growth has observed (1,1%) and the exact population amount yielded to 6.160 people compared to 6.088 people in last inventory of 2001 (Hellenic Statistical Authority, 2017).

The highest altitude of the study domain is 433 meters (DEM). The total area amounts to 4.887,7 ha, while the length of the coast is 44 km (skiathosisland.com, 2017).

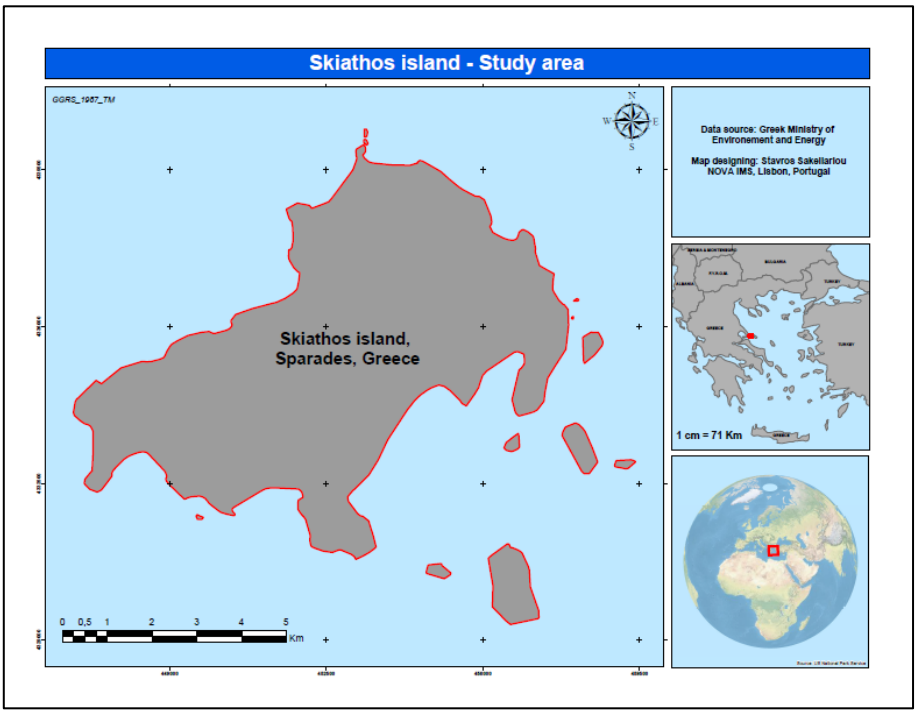

Figure 3.1. Geographical location of Skiathos in a nationwide and worldwide perspective

Source: Greek Ministry of Environment and Energy, 2017; own processing

3.2 Data

First of all, it should be mentioned that the adopted projection system is the corresponding Greek Geodetic Reference System 1987, called *GGRS_1987_Transcerse Mercator*.

One of the influential factors of forest fires phenomena is the geomorphology of the study area. The topography consists of three main dimensions, namely, the elevation, slope, and aspect. The discussion about the impact and interrelationship of these factors to forest fires ignition and propagation is described in the subsequent section (fire risk).

3.2.1 Elevation

The elevation dimension is derived from the Digital Elevation Model (DEM) (Figure 3.2). The DEM depicts the scalable fluctuation of elevation across the island.

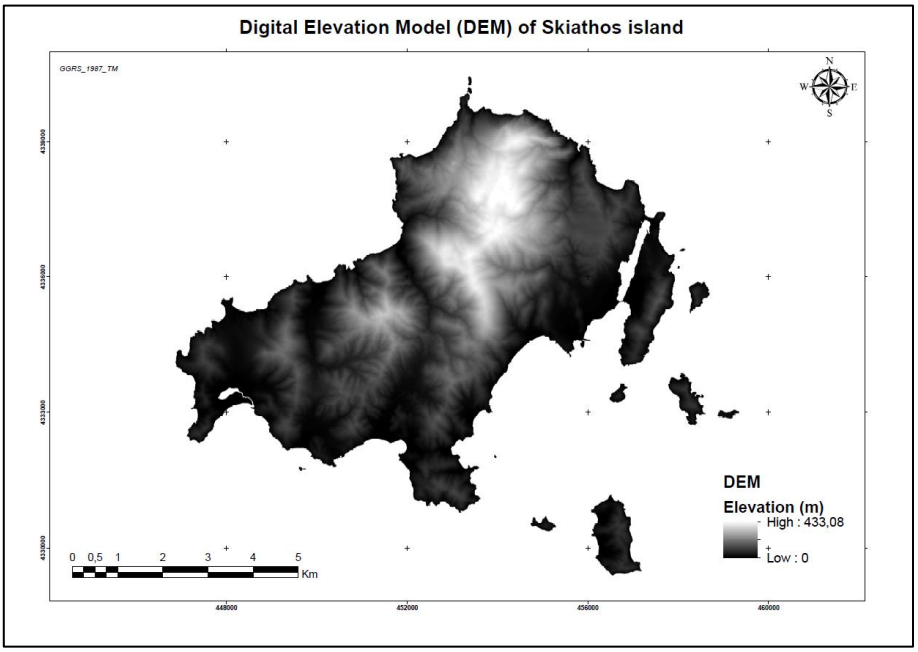

Figure 3.2. Digital Elevation Model of Skiathos

Source: NCMA, 2012; own processing

After the necessary geoprocessing and cartographic processes (*reclassify; conversion from raster to polygon; dissolve; zonal geometry as table etc.*), we created the following table (Table 3.1) which shows the elevation levels divided by distinct zones of 100 meters. As we may observe, the study domain is primarily occupied by lowland areas, followed by relatively small regions with higher altitudes. Specifically, the two first elevation zones (up to 200 m.) occupy 81% of the entire island, while the next two elevation zones (of medium height) occupy 18% of the study area.

Elevation levels (m)	Area (ha)	%
0 - 100	2872,2	58,8
101 - 200	1121,8	23,0

201 - 300	484,0	9,9
301 - 400	364,7	7,5
401 - 430	45,1	0,9
Total	**4887,7**	**100,0**

Table 3.1. Elevation zones

Source: NCMA, 2012; own processing

The Figure 3.3 presents the spatial allocation of all the aforementioned elevation zones.

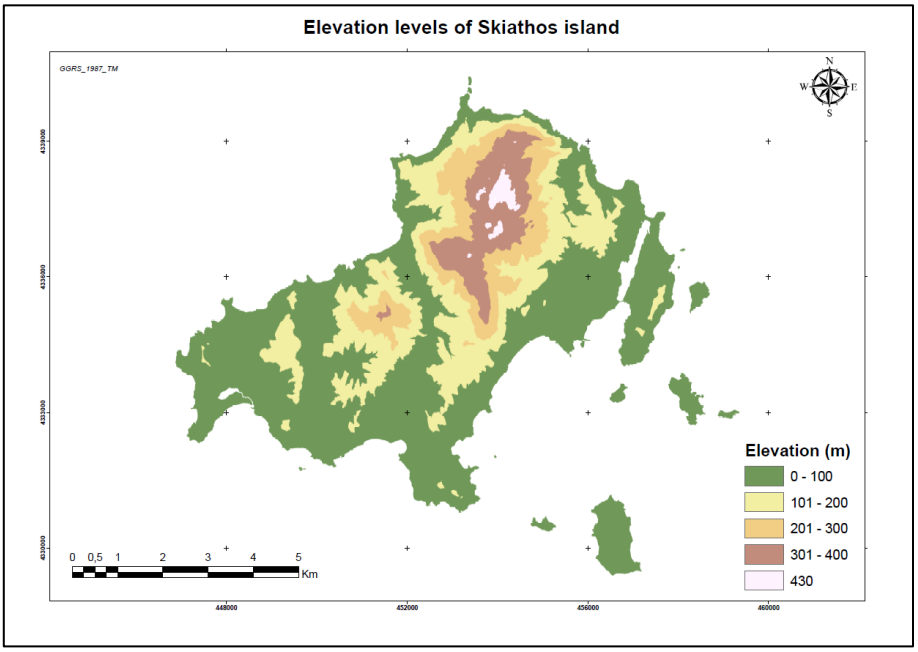

Figure 3.3. Elevation levels of Skiathos

Source: NCMA, 2012; own processing

3.2.2 Slope

Slope is another crucial factor that may drastically affect the fire propagation. Slope is stem from DEM and expresses "*the incline, or steepness, of a surface*" (Support.esri.com, 2017a).

After the essential geoprocessing and cartographic processes (*slope; reclassify; conversion from raster to polygon; dissolve, zonal geometry as table etc.*) we developed the following graph (Graph 3.1) which presents the slope levels per five degrees. As we may see, there is a trend of increasing area with higher slope up to 30% (85% of the entire study area), while a percentage of 14,5% corresponds to surfaces with slopes more than 30%. Hence, we realize that the slope factor may play a crucial role in fire propagation.

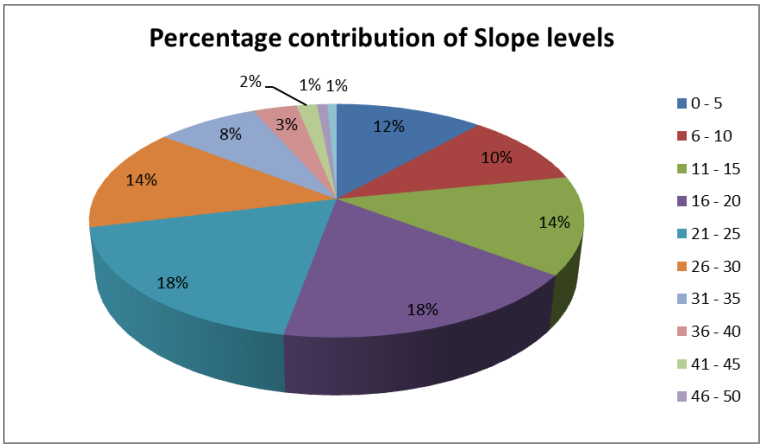

Graph 3.1. Slope levels

Source: NCMA, 2012; own processing

The Figure 3.4 depicts the spatial allocation of all the distinct slope zones (per 5 degrees).

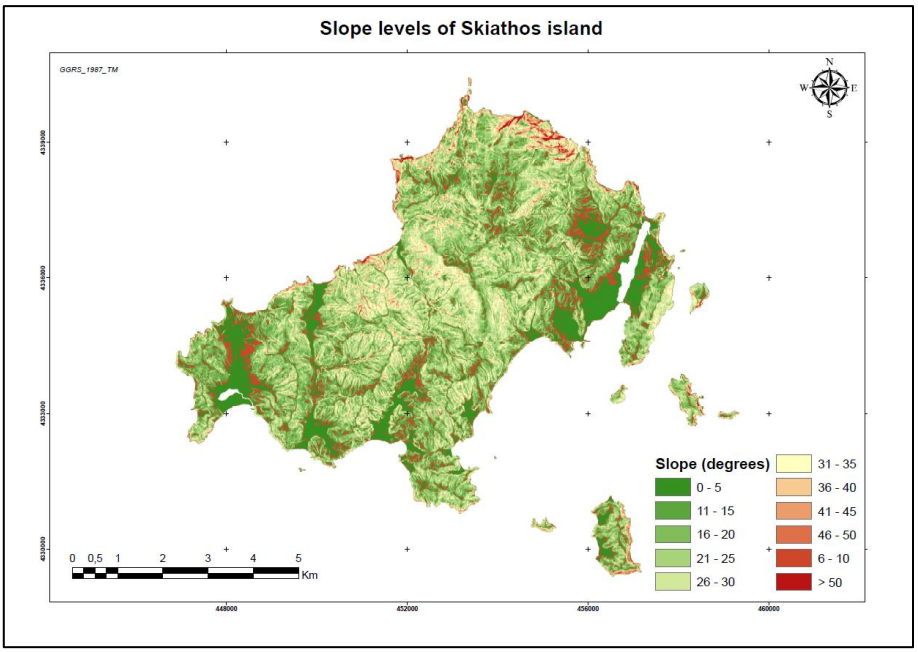

Figure 3.4. Slope levels of Skiathos

Source: NCMA, 2012; own processing

3.2.3 Aspect

Aspect is the last important topography factor that has distinct impact on forest fires events. By definition, aspect is "*the compass direction that a topographic slope faces, usually measured in degrees from north*" (Support.esri.com, 2017b).

After the essential geoprocessing and cartographic processes (*aspect; reclassify; etc.*) we created the following graph (Graph 3.2) which presents the aspect levels based on the surface direction. As we may observe, there is a relatively equal distribution among the different surface directions by almost

10% of the island on each direction. However, it should be noted that the most dangerous direction is related to south-facing surfaces. Consequently, we may see a total percentage of 38,1% of the study domain is covered by south-faced surfaces (including southwest and southeast aspect).

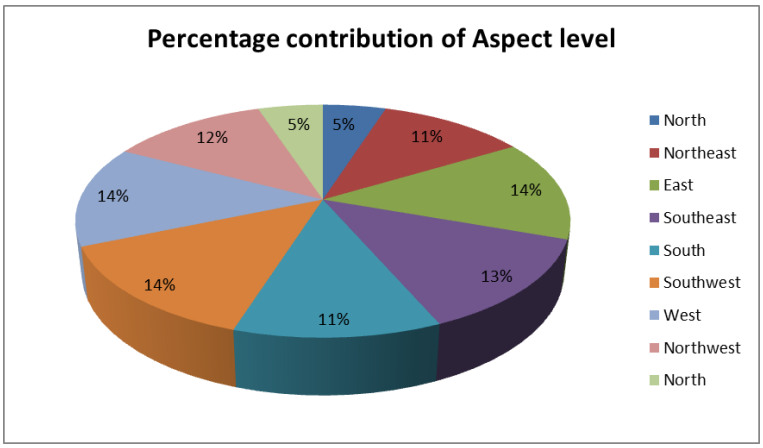

Graph 3.2. Aspect levels

Source: NCMA, 2012; own processing

The following map (Figure 3.5) depicts the spatial allocation of all the distinct aspect levels (based on different direction).

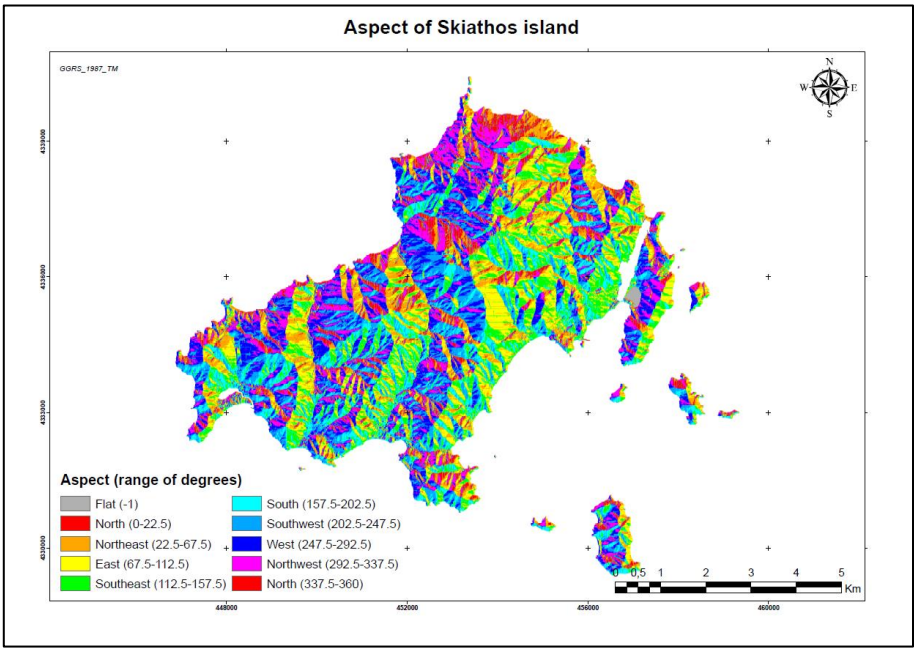

Figure 3.5. Aspect levels of Skiathos

Source: NCMA, 2012; own processing

3.2.4 Climatic characteristics

One of the most critical elements on forest fires phenomenon constitutes the climatic/meteorological conditions. When the climatic conditions are favorable to forest fires ignitions and spread, the fire risk

is getting higher and higher. Due to extremely small spatial scale of the study area, there is no any weather station on the surface of the island, hence, there is no updated and past records about the weather situation and evolution. However, due to the great significance of this dynamic variable, we adopted an alternative solution, taking the most crucial meteorological indices from the closest weather station. This station is located in the city of Volos which is the center of this administrative region. The exact geographic characteristics of the station are the following ones: Elevation: 52 m; Latitude: 39° 22' 31" N; Longitude: 22° 57' 32" E (Meteo, 2017a). The similarity of the weather conditions can be depicted from the small distance between the station and the study area, which amounts to 41 nautical miles (skiathosisland.com, 2017).

Even though we cannot directly include the climatic variables in the fire risk model because of the absence of any data or a reasonable allocation of a few weather stations (for spatial interpolation purposes), it is quite important to have a general image about the weather characteristics of the study area and their interrelation with forest fire events. In addition, we will try to adopt an indirect approach, estimating the situation of vegetation in terms of greenness and moisture for the month when most severe incidents take place.

The following tables present the main meteorological conditions for the fire season in Greece which is from June to September. In order to obtain a recent image and to get the vegetation indices in the riskiest month, we calculated the values for three consecutive years, namely, from 2015 to 2017. Thus, we get more reliable results decreasing the influence of any fluctuations in those years. The key variables examined were the mean and highest temperature per month; the maximum and minimum relative humidity (average values per month); the level of precipitation; and the wind characteristics (wind speed and direction).

As we can observe from the Tables 3.2 and 3.3, the riskiest months are July and August where the highest mean and high temperatures have been recorded; the lowest maximum and minimum relative humidity have been observed; the lowest level of precipitation has been noted and average wind speed took place. Therefore, we conclude that the riskiest month is August, when the lowest level of rainfall has been observed in conjunction with the lowest moisture. Hence, the combination of high temperatures and low levels of rainfall (and moisture subsequently) could easily lead to more frequent and severe forest fires phenomena.

Year	Month	Mean Temperature (C^o)	High Temperature (C^o)	Low Temperature (C^o)	Maximum Relative Humidity (%)	Minimum Relative Humidity (%)
Average 2015-2017	June	25,5	37,6	16,7	76,6	48,2
	July	28,0	38,7	18,6	71,3	43,0
	August	27,9	36,7	19,6	68,7	42,6
	September	24,0	36,7	15,5	82,5	56,5

Table 3.2. Temperature and humidity indices

Source: Meteo, 2017b, Own processing

Year	Month	Rainfall (mm)	Mean wind speed (km/hr)	High wind speed (km/hr)	Wind direction
Average 2015-2017	June	60,5	4,8	57,9	NE
	July	46,4	4,9	52,0	NE
	August	9,6	4,8	52,6	NE
	September	117,6	3,7	44,3	NE

Table 3.3. Precipitation and wind characteristics indices

Source: Meteo, 2017b, Own processing

The next figure (Figure 3.3) depicts the interrelationship of mean temperature and precipitation in the examined four months, confirming the combination of high temperatures and low levels of rainfall in July and August and especially in August. This fact inevitably leads to lower levels of moisture and more favorable conditions for forest fires ignition and propagation.

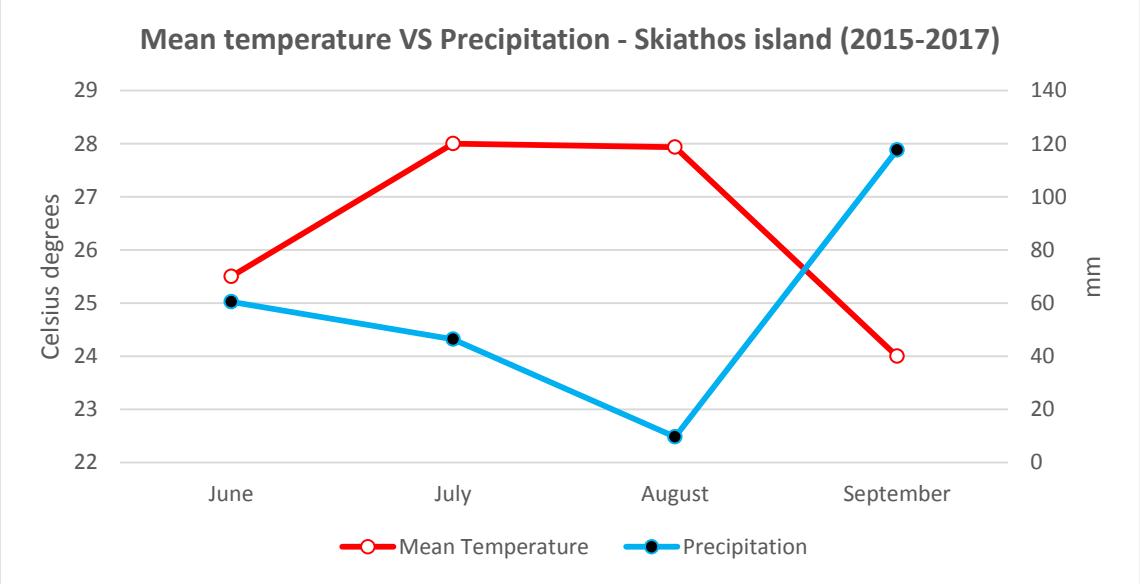

Figure 3.3. Mean temperature vs precipitation in Skiathos

Source: Meteo, 2017b, Own processing

Finally, the above conclusion has been confirmed from the fire history in national level. Specifically, according to a study conducted by Tsagari et al. (2011) 62% of the total fire ignitions have occurred from July to September which destroyed 85% of the total burned areas in Greece. Based on the findings of this study, 24% of the total fire ignitions and 36% of the total burned areas have occurred in August, which are the highest percentages in Greece from a time span from 1983-2008 (Tsagari et al., 2011).

3.2.5 NDVI 1990, 2016

NDVI is considered as one of the most prevalent indices in characterizing the vegetation conditions. The classification of NDVI can produce valuable information about specific characteristics of vegetation and the land cover. Specifically, NDVI ranges from -1 to +1 and can reveal some certain

features based on remote sensing techniques. Generally, values below 0,1 may describe non-vegetated regions, sandy surface or water bodies. The next interval of the spectrum (0,2 – 0,5) can capture features of vegetation leading to not dense species (shrubs, grasslands) and some types of crop cultivations, while the last interval (> 0,5) usually reflects to dense and healthy forest species (USGS, 2017). This, type of information (along with humidity indices like NDMI) plays a critical role in fire risk estimation.

In order to calculate the NDVI index for 2016, we used the following equation (for Landsat 8), exploiting the information of Red (R) and Near Infrared (NIR) bands (4 and 5 respectively) reflectance:

NDVI = (NIR – R) / (NIR) + R): landsat.usgs.gov, 2017

So, after the retrieval and the processing of the corresponding bands (*clip; projection; math algebra etc.*), we created the NDVI map along the study area, as depicted in the next map (Figure 3.6). The most appropriate image taken on August 12th, 2016, without cloud interference. The selection of the month was based on the climatic information described in the previous section.

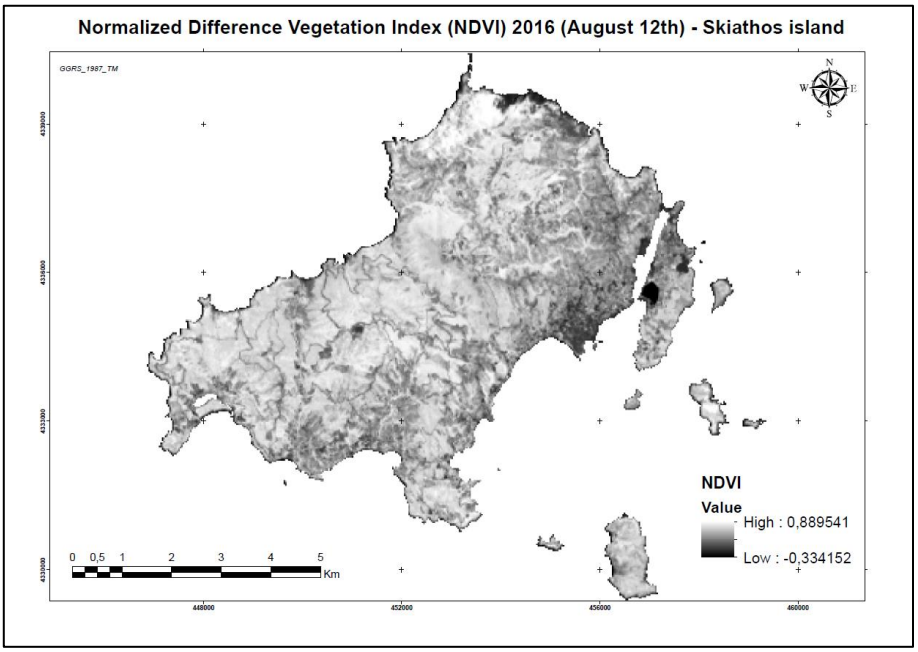

Figure 3.6. NDVI of Skiathos (2016)

Source: USGS - Earth Explorer 2017, own processing.

In order to make the image clearer (Figure 3.7), we adopted the classification as explained above. Thus, we may observe that the lowest interval of spectrum primarily includes the artificial structures (urban areas), sandy-arid surface and possibly water bodies. The next interval incorporates the agricultural land which thrives close to the inhabited areas and the easily accessible coastal regions, while the last interval includes many types of forest that dominate the majority of the island. Definitely, here we take advantage of the vegetation condition information (and not the discrimination of land cover), since this type of information is crucial in fire behavior.

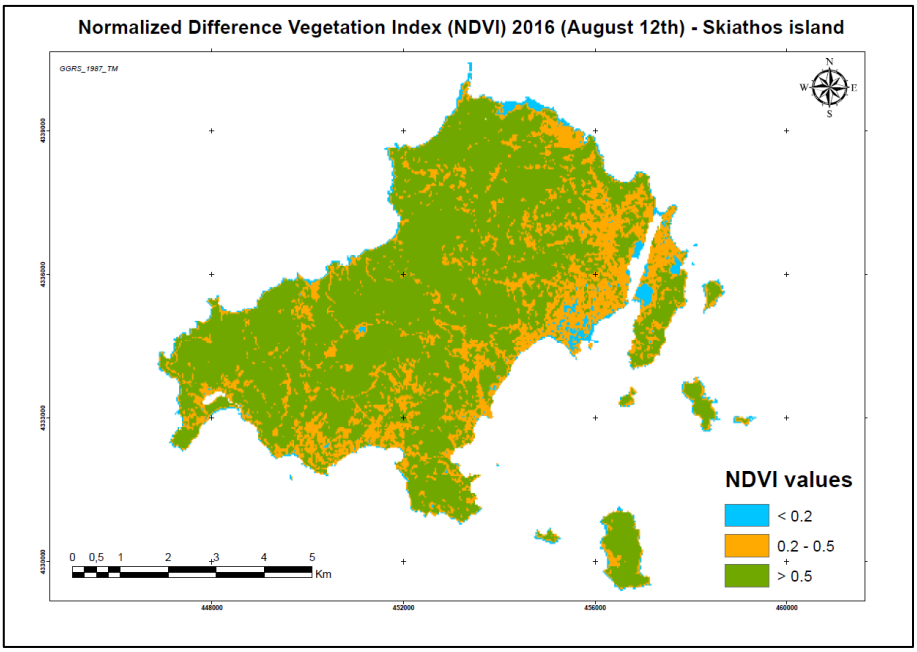

Figure 3.7. Reclassified NDVI of Skiathos (2016)

Source: USGS - Earth Explorer 2017, own processing.

In the following table (Table 3.4), we see the area occupied by each predefined interval of the spectrum. Reasonably, most of the area belongs to the last class, since forested land is the dominant land cover on the island.

Interval	Area (ha)	%
< 0,2	176,67	4%
0,2 - 0,5	1.204,65	25%
> 0,5	3.507,21	72%
Total	4.888,53	100%

Table 3.4. Area per NDVI interval (2016)

Source: USGS - Earth Explorer 2017, own processing

In the case of NDVI for 1990, the Landsat 5 Thematic Mapper sensor was used. In order to calculate this index, we used the following equation (for Landsat 5), exploiting the information of Red (R) and Near Infrared (NIR) bands (3 and 4 respectively) reflectance:

NDVI = (NIR – R) / (NIR) + R): landsat.usgs.gov, 2017

So, after the retrieval and the processing of the corresponding bands (*clip; projection; etc.*), we proceeded to another necessary procedure, namely, the radiometric calibration of the involved bands.

Firstly, we transformed the Digital Number of each band to radiance through *Gain and Bias Method* adopted the following equation (Center for Earth Observation, 2017):

Li = gain * DN + bias,

Where:

Li: is the cell value as radiance

DN: is the cell value digital number

Gain: is the gain value for a specific band

Bias: is the bias value for a specific band

So, the first transformation that took place was (we computed the radiometric calibration for the 5th band as well because it will be need for the next index, called NDMI)[1]:

Li_Band 3: (1.043976 * DN) + (-2.21)

Li_Band 4: (0.876024 * DN) + (-2.39)

Li_Band 5: (0.120354 * DN) + (-0.49)

Following, we had to transform the radiance to Top of Atmosphere Reflectance, based on the following equation (Center for Earth Observation, 2017):

$Ri = pi * Li * d^2 / ESUNi * \cos(thita_s)$,

Where:

Ri: Unitless plantary reflectance

Li: spectral radiance (from earlier step)

d: Earth-Sun distance in astronmoical units

ESUNi: mean solar exoatmospheric irradiances[2]

$thita_s$: solar zenith angle

Hence, the respective equations applied to each band are the following ones:

Band 3: (3.14 * Li_Band3 * (1.0116265 * 1.0116265)) / 1551 * Cos(90-51.57122754)

Band 4: (3.14 * Li_Band4 * (1.0116265 * 1.0116265)) / 1036 * Cos(90-51.57122754)

Band 5: (3.14 * Li_Band5 * (1.0116265 * 1.0116265)) / 214.9 * Cos(90-51.57122754)

Finally, we proceeded to the math algebra of all these transformed bands based on the initial equation presented in the beginning of the current section. Thus, we created the NDVI map along the study area, as depicted in the next map (Figure 3.8). The most appropriate image taken on August 21st, 1990, without cloud interference. The selection of the month was based on the climatic information described in previous sections.

[1] The gain and bias values were retrieved from Chander et al. (2009).
[2] These values were retrieved from https://landsat.usgs.gov/esun, 2017

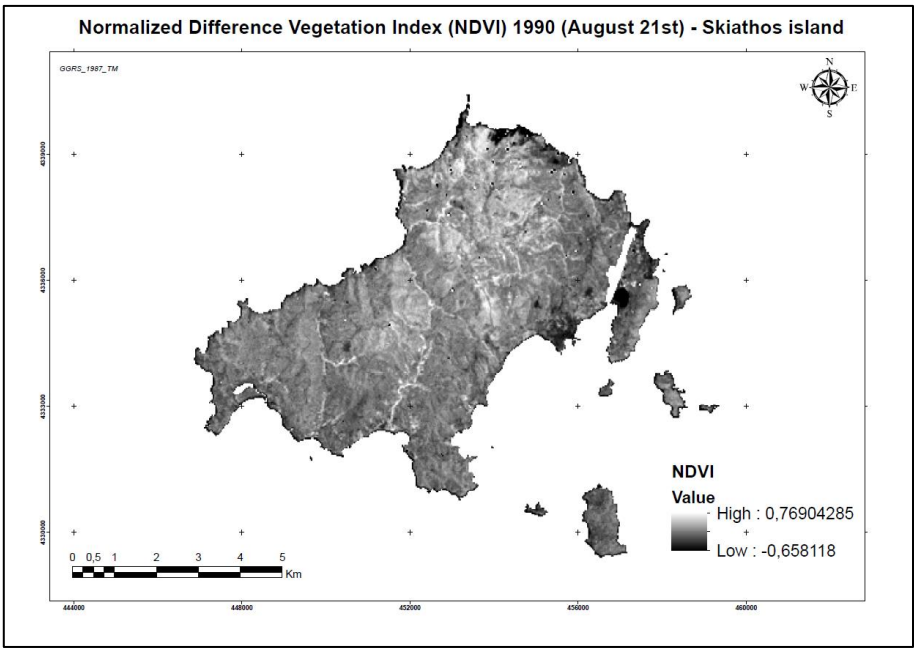

Figure 3.8. NDVI of Skiathos (1990)

Source: GloVis 2017, own processing

For comparison reasons, we adopted the same classification scheme as we did for the same index in 2016 (Figure 3.9).

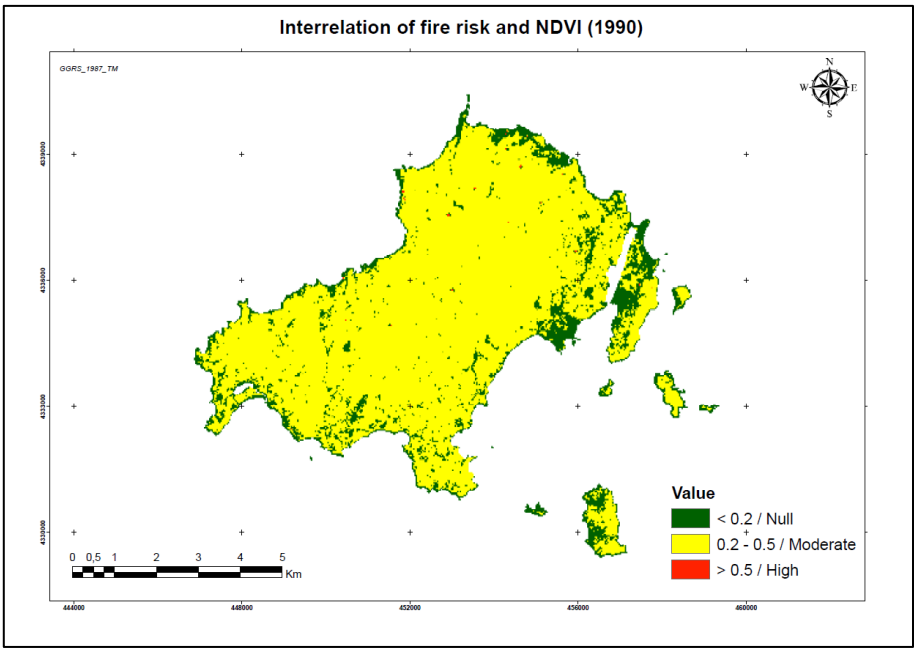

Figure 3.9. Reclassified NDVI of Skiathos (1990)

Source: GloVis 2017, own processing

As we observe from the above map (Figure 3.10), the majority of the island is covered by agricultural fields and shrubs as well as not dense forested areas. Here, it should be highlighted the fact that there is a possibility of some errors in the bands, since we expected to have more extensive regions of more

than 0.5 NDVI value (dense forest), due to the existence of many forested territories in the study domain (Table 3.5).

Interval	Area (ha)	%
< 0.2	731	15%
0.2 - 0.5	4.155	85%
> 0.5	3	0%
Total	**4.889**	**100%**

Table 3.5. Area per NDVI interval (1990)

3.2.6 NDMI 1990, 2016

Another critical factor is the NDMI index, especially under the great shortage of the relative data in our case study. This kind of information is vital, since it is related with one of the most important factors of fire weather, namely, the humidity. Consequently, the higher the degree of moisture, the less possibilities for extensive and destructive forest fire events.

In order to calculate the NDMI index for 2016, we used the following equation (for Landsat 8), exploiting the information of Near Infrared (NIR) and Shortwave Infrared (SWIR) bands (5 and 6 respectively) reflectance:

NDMI = (NIR – SWIR) / (NIR + SWIR): landsat.usgs.gov, 2017

On this map (Figure 3.10), we can conclude that the regions that are affected from water stress are mainly the urban/artificial surface/structures and some agricultural lands which require water on the summer season. On the contrary, positive values are concentrated on forests that reserve more moisture on their territory.

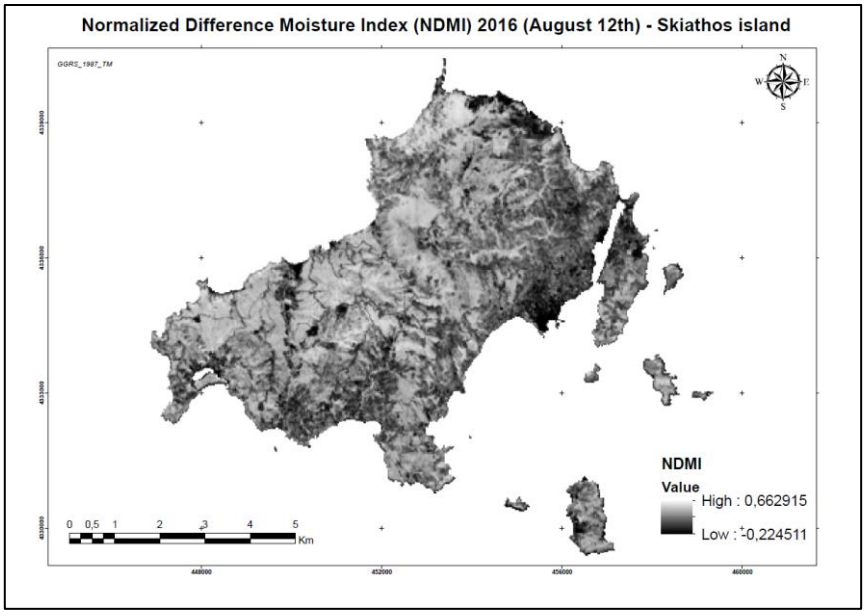

Figure 3.10. Reclassified NDMI of Skiathos (2016)

Source: USGS - Earth Explorer 2017, own processing.

After the radiometric calibration of all the involved bands in order to calculate the NDMI index for 1990, we used the following equation (for Landsat 5), exploiting the information of Near Infrared (NIR) and Shortwave Infrared (SWIR) bands (5 and 6 respectively) reflectance:

NDMI = (NIR – SWIR) / (NIR + SWIR): landsat.usgs.gov, 2017

On this map (Figure 3.11), we can conclude that the regions that are affected from water stress are mainly the urban/artificial surface/structures and some agricultural lands which require water on the summer season. On the contrary, positive values are concentrated on forests that reserve more moisture on their territory.

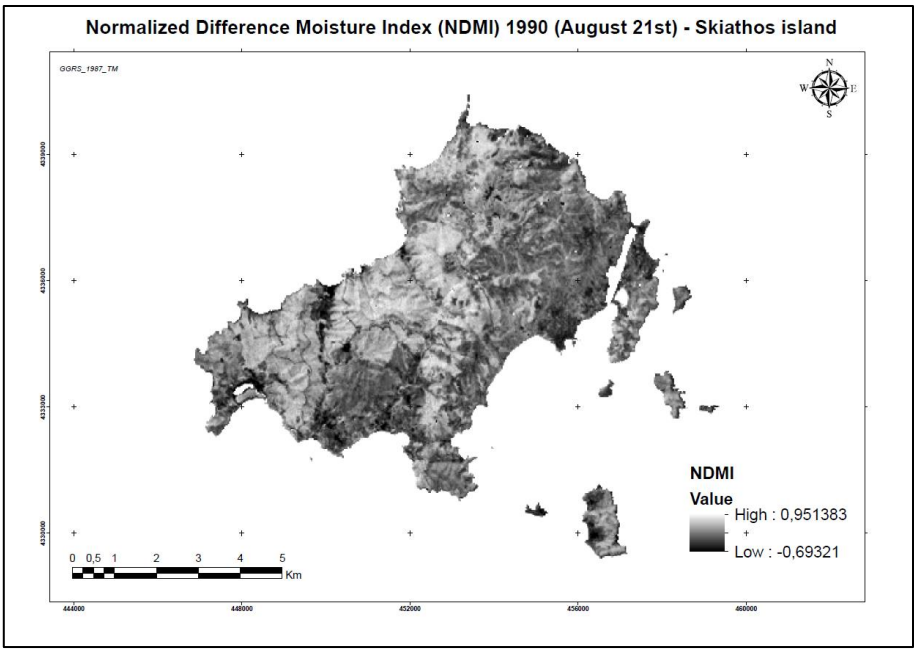

Figure 3.11. NDMI of Skiathos (1990)

Source: GloVis 2017, own processing

3.2.7 Land cover/use 1990, 2012

Another very important input in fire modeling is the fuel. Fuel is the most appropriate and important input in any fire simulation software, because it describes the potential fire behavior. However, due to the shortage of this kind of data for our study area, we used substitute of fuels, namely, the land cover of the island. This specific input is used to estimate the risk of igniting and possible fire spread across the study domain. In addition, due to the dynamic nature of land cover (subject to changes in a certain timeframe), we examined the land cover statistics, allocation and evolution from 1990 to 2012, using the respective land cover layers (1990 and 2012).

The technical characteristics of the Corine Land Cover (CLC) layers are determined by "*44 classes in nomenclature, 25 hectares minimum mapping unit and 100 meters minimum mapping width and are distributed in the standard European Coordinate Reference System defined by the European Terrestrial Reference System 1989 (ETRS89) datum and Lambert Azimuthal Equal Area (LAEA) projection (EPSG: 3035)"* (land.copernicus.eu, 2017). We decided to use these maps instead of

classifying the respecting satellite images for many reasons, but the most important ones are: the high level of detail in vegetation species which plays a crucial role in fire behavior; the high degree of validity derived from the European Environmental Agencies and the interconnection with the examined fire history as described in the methodology section.

We mentioned that we tried to estimate the fire risk evolution through these time steps, on the grounds that we obtained the road network database for these specific years (1995 and 2016). To this end, we used the corresponding NDVI and NDMI thematic maps and indices for the same years.

In order to get the essential images with the land cover information, we retrieved the data and a number of geoprocessing procedures took place. Indicatively, we had to re-project the data to our projection system; we clipped the entire image according to our study domain; we re-organized the land cover types (calculate area in ha; reclassify layers; cartographic refinement etc.).

The next table (Table 3.6) presents the land cover structure based on 1990 data. As we may see, 53,5% of the entire island is covered by different types of forest; 45,5% of the study area is occupied by agricultural areas, while only 1% of the island is occupied by artificial structures. It should be understood, that there is a significant percentage of the riskiest inputs for forest fires ignition and extended spread, since only coniferous and mixed forests along with transitional woodland-shrub occupy almost 40% of the entire island.

CLC_CODE	Land_cover	Area_Ha	%
112	Discontinuous urban fabric	46	1,0
124	Airports	5	0,1
223	Olive groves	337	7,1
242	Complex cultivation patterns	152	3,2
243	Agriculture and natural vegetation	1682	35,2
311	Broad-leaved forest	361	7,6
312	Coniferous forest	1440	30,2
313	Mixed forest	100	2,1
321	Natural grasslands	44	0,9
323	Sclerophyllous vegetation	208	4,4
324	Transitional woodland-shrub	362	7,6
333	Sparsely vegetated areas	37	0,8
	Total	4774	100,0

Table 3.6. Area per land cover type (1990)

Source: land.copernicus.eu, 2017, own processing

The following map (Figure 3.12) shows the spatial allocation of all the aforementioned land cover types in the island of Skiathos in 1990.

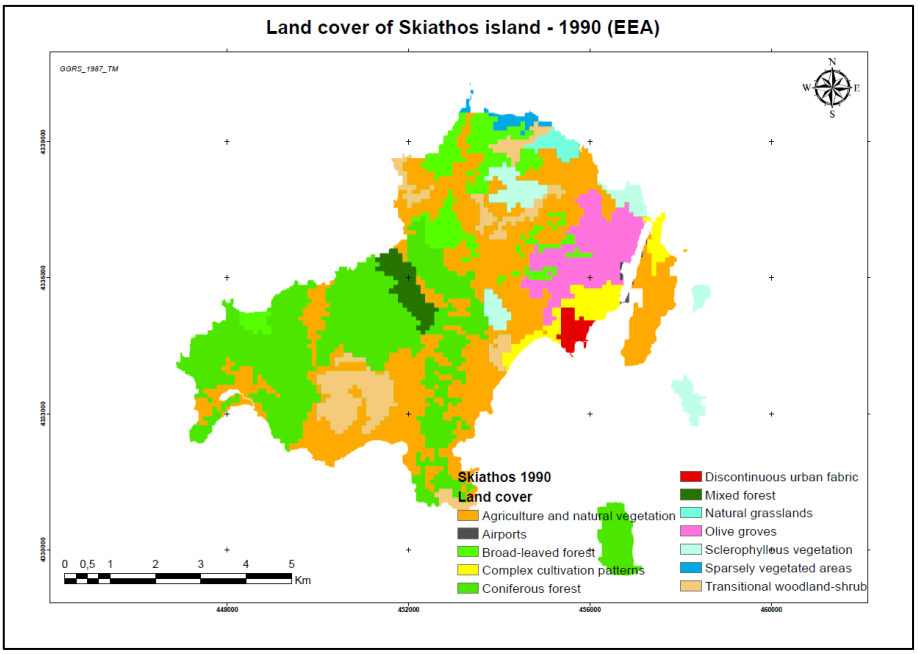

Figure 3.12. Land cover types of Skiathos (1990)

Source: land.copernicus.eu, 2017, own processing

The next table (Table 3.7) shows the land cover structure based on 2012 data. As we may see, 53,9% of the entire island is covered by different types of forest; 44,9% of the study area is occupied by agricultural areas, while only 1,1% of the island is occupied by artificial structures. It should be understood, that there is a significant percentage of the most risky inputs for forest fires ignition and extended spread, since only coniferous and mixed forests along with transitional woodland-shrub occupy more than 40% of the entire island.

CLC_CODE	Land_cover	Area (Ha)	%
112	Discontinuous urban fabric	45	0,9
124	Airports	10	0,2
223	Olive groves	335	7,1
242	Complex cultivation patterns	138	2,9
243	Agriculture and natural vegetation	1658	34,9
311	Broad-leaved forest	362	7,6
312	Coniferous forest	1443	30,4
313	Mixed forest	103	2,2
321	Natural grasslands	43	0,9
323	Sclerophyllous vegetation	206	4,3
324	Transitional woodland-shrub	370	7,8
333	Sparsely vegetated areas	34	0,7
	Total	**4747**	**100,0**

Table 3.7. Area per land cover type (2012)

Source: land.copernicus.eu, 2017, own processing

The next map (Figure 3.13) shows the spatial allocation of all the aforementioned land cover types in the island of Skiathos in 2012.

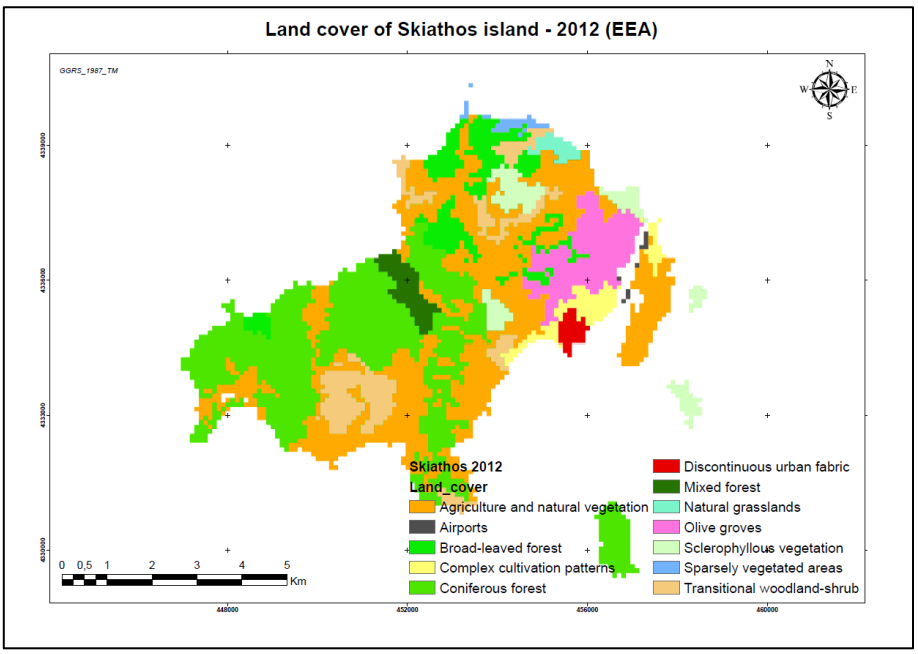

Figure 3.13. Land cover types of Skiathos (2012)

Source: land.copernicus.eu, 2017, own processing

Finally, the last table (Table 3.8) of this section presents the percentage change of each land cover for our study area (1990-2012).

Land_cover	% change (1990-2012)
Discontinuous urban fabric	-2,80
Airports	121,35
Olive groves	-0,61
Complex cultivation patterns	-9,34
Agriculture and natural vegetation	-1,43
Broad-leaved forest	0,26
Coniferous forest	0,23
Mixed forest	3,04
Natural grasslands	-1,78
Sclerophyllous vegetation	-1,07
Transitional woodland-shrub	2,16
Sparsely vegetated areas	-8,35

Table 3.8. Per cent change of area per land cover type (1990 - 2012)

Source: land.copernicus.eu, 2017, own processing

From the Table 3.7, we observe that urban areas have been decreased, a fact that might be due to classification errors, since the trend is quite opposite. It should be highlighted that agricultural regions have been reduced by almost 11%, most probably in favor of artificial structures. In the same context,

the total forested area (including all the relative land cover types – CLC=3), we see that a percentage of 5.5% of the specific land cover has been lost. This fact is absolutely in line with the most recent forest fires that destructed 265 ha (5,5% of the island) in 2007, as we describe many details in the following sections.

Hence, most importantly, because Corine Land Cover data have been created in coarse resolution (100 m.), most of the individual artificial structures have been misclassified. To this end, we used historical databases and orthophotos in order to incorporate this crucial dimension in the land cover maps, which consist one of the most crucial inputs in fire modeling. This process corrected the real existence of all artificial structures between the two dates.

3.2.8 Road network 1996, 2016

The road network constitutes one more vital factor in fire risk modeling, since many incidents ignite on the areas nearby of roads due to accidental reasons (e.g. cigarettes, barbecue in the countryside), arsons etc. To this end, it is considered meaningful to describe the dense network and its evolution from 1996 to 2016.

The first table (Table 3.9) shows the road network structure per type in 1996. We observe that a total road network of 258,9 km. crosses such a small territory. Due to the nature of island, almost half of the total road network falls into forest type category highlighting the domination of this specific land cover. The remaining percentages fluctuate in reasonable levels.

Road type	Length (m.)	%
Primary road	31.259	12,1%
Residential road	25.309	9,8%
Service road	72.440	28,0%
Forest road	129.707	50,1%
Total	**258.715**	**100,0%**

Table 3.9. Area per road network type (1996)

Source: Samara, 2016, own processing

The following map (Figure 3.14) depicts the structure and spatial allocation of residential and road network along the study area in 1996.

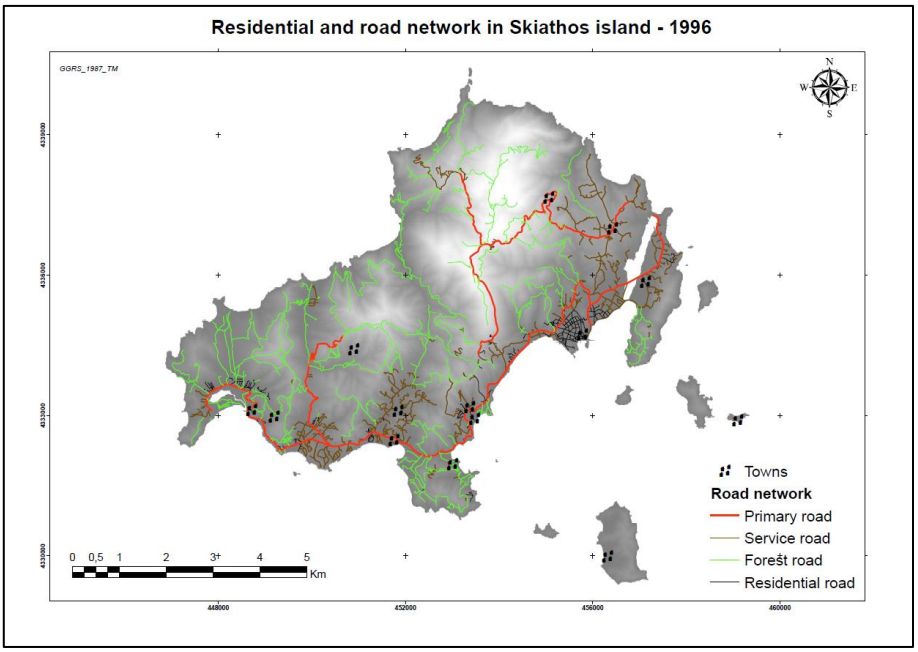

Figure 3.14. Road network of Skiathos (1996)

Source: Samara, 2016, own processing

The second table (Table 3.10) shows the road network structure per type in 2016. We observe that a total road network of 227,6 km. crosses the island. Here, it should be highlighted that the differences with the previous table are due to several factors, such as: i) different types of classification because the data are coming from totally different sources; ii) subjectivity in classification processes, since we can see large divergence in specific road types. For instance, in the second case, some types of service roads may consist of forest roads in the first case and vice versa; iii) indeed, some road segments might have been abolished through time. However, it should be emphasized that we focused on the proximity of road network itself (any type) for the aims of our project. We did this because the critical factor is the proximity and accessibility themselves and not the specific type of road network. Nevertheless, we had to describe the situation of road network on the island in order to get a better image.

Road type	**Length (m.)**	**%**
Primary road	35.360	15,5%
Residential/service road	97.147	42,7%
Forest road	80.629	35,4%
Footway/path	14.456	6,4%
Total	**227.592**	**100,0%**

Table 3.10. Area per road network type (2016)

Source: Geofabrik 2016, own processing

Finally, the next map (Figure 3.15) shows the structure and spatial allocation of residential and road network along the study domain in 2016.

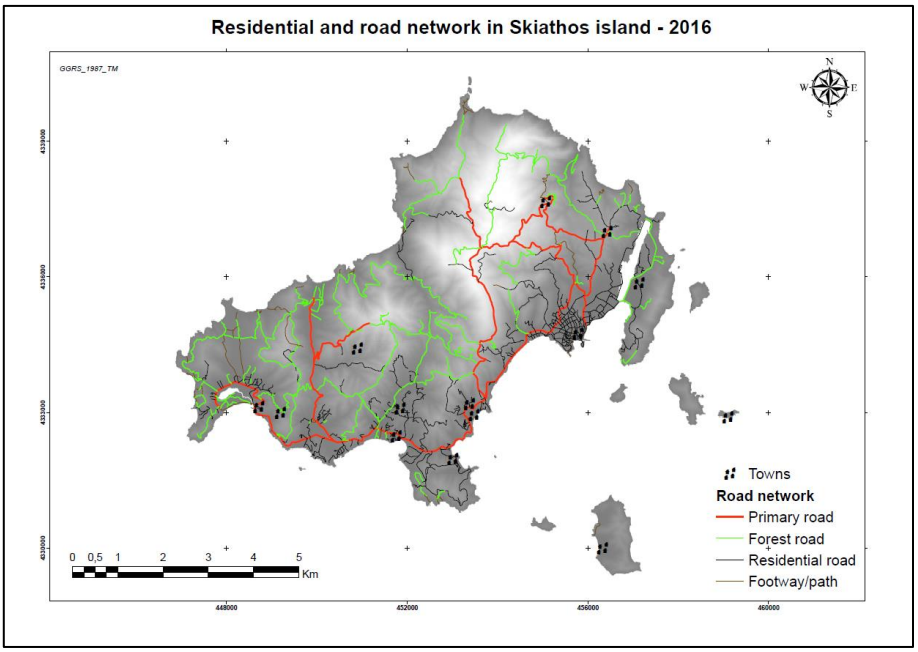

Figure 3.15. Road network of Skiathos (2016)

Source: Geofabrik 2016, own processing

3.2.9 Fire history

Skiathos island has faced four intense forest fires events in almost twenty years, from 1984 to 2016. The most affected land covers consisted of *Transitional woodland-shrub*, *Coniferous forest*, and *Mixed forest.* The Table 3.11 depicts the fire history of the island highlighting the allocation of each land cover in absolute and relative numbers.

Year	CLC type	Area burned in ha	%
1986	Coniferous forest	7,2	5,4%
	Transitional woodland-shrub	88	66,3%
	Other	37,5	28,3%
	Total	**132,7**	
1999	Coniferous forest	4,2	1,9%
	Transitional woodland-shrub	176	79,1%
	Other	42,4	19,0%
	Total	**222,6**	
2000	Mixed forest	56,1	63,3%
	Transitional woodland-shrub	7,2	8,1%
	Other	25,3	28,6%
	Total	**88,6**	
2007	Coniferous forest	114,2	43,1%
	Transitional woodland-shrub	68,9	26,0%
	Other	82,1	31,0%
	Total	**265,2**	

Table 3.11. Area burned per land cover type

Source: NOA, 2017; Own processing

Even though the characteristics of the fire regime cannot be determined in such a small spatial scale, we can have an indication about the fire conditions in the island. In order to understand the significance of adopting efficient fire prevention measures, it should be emphasized the fact that in the above timeframe, almost 710 ha of burned area has been recorded which is equivalent of almost 15% of the entire island.

3.3 Methodology

3.3.1 Fire risk modelling

The corner stone of our methodology is primarily relied on the multi-criteria decision analysis. This framework applied not only for the fire risk estimation and the corresponding evolution, but for visibility analysis as well, determining the most suitable locations for the establishment of a certain number (as least as possible) of watchtowers. The theoretical background of the study was developed in the literature review section.

Briefly, the purpose of the study can be characterized of multiple nature. The first objective is focused on the exploration of the impact of the natural (topography, land cover, vegetation condition and moisture) and anthropogenic factors (proximity from anthropogenic structures) to forest fire ignition and propagation. All these factors have their distinct added value to fire incidents and fire behavior as we will see in the following sections. It should be mentioned, that we use fire hazard and fire risk terms interchangeably in this study for simplicity purposes.

It should be highlighted that the selection of all these factors has been conducted based on their influence on forest fires phenomenon. Generally, it is known that due to the nature of each contributing factor, natural dimensions are more related to fire behavior, while the fire ignition pattern is more correlated to human factor. This is happening because the most frequent cause of a forest fire event is derived from humans (either by accident or on purpose). The mix of certain land covers, such as forest and urban areas (Wildland Urban Interface) increases the possibilities of a fire incident to occur (Chas-Amil et al., 2013). Especially in Greece, there are many cases of burning the agricultural fields and pastures for obvious reasons and these events may be expanded to forested areas with unexpected implications.

Slope is a dominant factor that affects the fire acceleration and as the steepness increases so does the fire spread. That is the result of multiple interacting factors such as: the immediate proximity of fuels to the fire; the consequent reduction of moisture levels and the impact of wind that makes the fire expand more quickly. Aspect is another factor that influences forest fires. Generally, southern aspects are characterized by higher temperatures, decreasing the moisture of the ground and fuels, providing favorable conditions to the fire expansion (Environment and Natural Resources, 2017). Elevation is

related with where most fire incidents take place. This factor is similar to accessibility. There are some certain elevation zones where most fire ignitions occur (the lowest regions) and others that (most frequently) only natural cause may trigger a fire ignition (the highest regions).

Regarding the association of land cover and fire risk, we adopted a differentiated approach based not only on the endogenous characteristics of each land cover type, but also taking into consideration real fire statistics in similar fire regimes like the South European Mediterranean countries. Hence, we supported our argument based on a study conducted by *Pereira et al.* (2014) who estimated the fire proneness of each land cover type. The foundation of this study was relied on the detailed exploration of fire statistics and the interrelation with the Corine Land Cover in South Europe, where the countries of this region have been most affected by forest fires. Hence, besides a certain number of fires statistics indices examined, they calculated the fire proneness index based on the interrelation of burnt area per specific land cover accompanied with the temporal evolution of this index from 2000 to 2012. Finally, they classified the land cover types based on their fire proneness, relied on real fire statistics for a time frame of 12 years and not only on the characteristics of each land cover itself (Pereira et al., 2014). This is very important, due to the fact that there might be some specific land cover types (e.g. coniferous forest) that could theoretically yield the most destructive results (in terms of fire intensity), but these regions might be less accessible or most protected (e.g. establishment of fire breaks etc.). So, we can face less burnt area and fewer fire ignitions on these specific land cover types compared to others (shrubs etc.). This is confirmed by *Pereira et al.* 2014, except the cases of enormous forest fires, which is a rational result of extensive fire events burning the most vulnerable fuels like coniferous forests. Similar classification was adopted by *You et al.* (2017), regarding the forest fuels susceptibility.

Pasture and agricultural land are classified as low fire risk, since the incidents of these areas are easily visible due to their spatial arrangement close to towns and roads as well as due to their limited fuel load. Urban areas are classified below the moderate risk, because they are related with many activities that could ignite forest fires and on the other hand, there is a mixture of land covers due to the Wildland Urban Interface. The most influential land covers are definitely related with forest fuels, namely, shrubs, broadleaved, coniferous forest etc. with a scalable degree of fire risk, depending on the structure and characteristics of forest fuel (density, canopy closure etc.).

Another important factor constitutes the fire weather. The fire weather is the interaction of three primary climatic conditions, such as temperature, moisture and wind characteristics. These factors heavily affect the fire environment (Environment and Natural Resources, 2017). As previously mentioned, due to the shortage of climatic data on this very local scale, we tried to use remotely sensed data to determine at least the condition and humidity of the vegetation (calculating the NDVI and NDMI indices respectively). We proceeded to this technique, since experienced agencies cite "*humidity is an important factor in firefighting, since wet and most green fuels will not burn freely*" (Environment and Natural Resources, 2017). Thus, it should be highlighted that these indices have

great impact on fire behavior and propagation through their corresponding characteristics (dense forests; grass and shrubs, arid surfaces, levels of moisture that affect the fire ignition and spread etc.). Specifically, the scale of NDVI and the respective risk was estimated based on the conditions (healthy or dead) and greenness of vegetation. Hence, the first interval (-0,33 – 0,2) may include non-flammable regions (water bodies, sandy surfaces, rocks etc.); the intermediate interval (0,2 – 0,5) primarily includes agricultural land and possibly some parts of shrubs and natural grasslands which are the most affected based on the previous analysis (land cover dimension). To this end, a moderate fire risk was assigned to this mixed class. The last interval incorporates dense forest with relatively high risk (dense forests with plenty of fuels) (USGS, 2017). On the other hand, the NDMI index and the corresponding risk are proportionally related with the amount of water/humidity captured by the ground. Again, we excluded the most extreme values (extremely high) because of the existence of some artificial structures which are inevitably shown areas with low humidity and affect the real purpose of the index and might slightly affect the final risk map.

Finally, the estimation of anthropogenic impact was conducted by establishing distinct zones along the road network and the urban region. These zones depict differentiated degrees of fire risk, since they are related on the one hand with accessibility issues (accidents; ignitions on purpose-arsons that each type of road permits) and on the other hand, with the number of socioeconomic activities that take place in the adjacent to urban land cover areas.

The Table 3.12 depicts the assignment of each factor to the corresponding fire risk based on a specific weight which reflects the hazard within each class. The determination of the classes for each factor are based on the key studies of the same field, as depicted in the Table 3.12 for each factor. Definitely, there is a light degree of a necessary adaptation (no significant changes) in the classes in order to reflect the local conditions of the island more reliably. For instance, the fire risk in relation to aspect is different in the north and south hemisphere. Moreover, the maximum distance from roads or towns was adjusted accordingly, since the study area is a small island. It is pointless to adopt greater distances for these structures. Consequently, the respective fire risk has been adjusted accordingly. In addition, the weighting scale was adjusted from 1 to 10 (instead of 1 to 5 like in many studies), because we considered that a more detailed fire risk map could be created, taking into account even minor changes (e.g. aspect factor). The source for the classification scheme for each dimension is shown beneath each factor in parenthesis.

Slope [degrees] (Eugenio et al. 2016, adapted)	**Weight**	**Fire Hazard**	**Aspect** (Saglam et al. 2008; Sharma et al. 2012, adapted)	**Weight**	**Fire Hazard**
0 – 5	1	Very low	Smooth ground	1	Null
5 – 15	3	Low	North	2	Very low
15 – 25	5	Moderate	Northeast	3	Low
25 – 35	7	High	Northwest	4	Lower than mean
35 – 45	9	Very high	East	5	Moderate

> 45	10	Extremely high	Southeast	6	Higher than mean
			West	4	Lower than mean
			Southwest	8	Very high
			South	10	Extremely high
Elevation [meters]	**Weight**	**Fire Hazard**	**Distance from roads [meters]** (Jaiswal 2002; Sivrikaya et al., 2014, adapted)	**Weight**	**Fire Hazard**
0 -100	10	Extremely high	400 - 500	2	Low
100 – 200	8	Very high	300 - 400	5	Moderate
200 – 300	5	Moderate	200 - 300	7	High
> 300	2	Low	100 - 200	8	Very high
			0 - 100	10	Extremely high
Land Uses (Pereira et al. 2014; You et al. 2017, adapted)	**Weight**	**Fire Hazard**	**Distance from towns [meters]** (Saglam et al. 2008; Sharma et al. 2012, adapted)	**Weight**	**Fire Hazard**
Airports; Discontinuous urban fabric	1	Very low	800 – 1000	2	Very low
Land principally occupied by agriculture, with significant areas of natural vegetation; Olive groves; Complex cultivation patterns; Sparsely vegetated areas	3	Low	600 – 800	3	Low
Broad-leaved forest	5	Moderate	400 - 600	5	Moderate
Coniferous forest	7	High	200 – 400	7	High
Mixed forest	8	Very high	0 - 200	8	Very high
Natural grasslands	9	Very high			
Sclerophyllous vegetation; Transitional woodland-shrub	10	Extremely high			
NDVI (values) (USGS, 2017)	**Weight**	**Fire Hazard**	**NDMI (values)** (Nurdiana & Risdiyanto, 2015)	**Weight**	**Fire Hazard**
-0,33 – 0,2	0	Null	> 0,3	1	Very low
0,2 – 0,5	5	Moderate	0,15 – 0,3	4	Moderate
> 0,5	7	High	0 – 0,15	7	High

	-0,22 – 0	9	Very high

Table 3.12. Knowledge-based ranking of the key factors to fire risk

Finally, besides the determination of an internal weight which interrelates the effect of each factor to forest fire risk, we assigned an extra (general) weighting factor to each distinct dimension which reflects the general significance to either forest fire ignition or propagation (here these characteristics are merged and present the total fire hazard)[3]. Hence, the land cover factor received a weight of five (the highest), since fires need the "appropriate" fuel in order to ignite and expand; the dimension of aspect received the weight of three due to its importance, especially at the Mediterranean ecosystems, receiving higher temperatures and decreasing the respective moisture levels; the slope factor that heavily affects the fire propagation receives the weight of two; the elevation dimension, which is based on fire history statistics, received the weight of one; the NDVI index received the weight of two and NDMI the weight of three; the distance from any type of road took the weight of two, since many roads cross large areas of forest and favorable territories to fire ignition; finally, the distance from urban areas took the weight of one, because even though many activities happen in these regions, fire incidents could be more easily discernible from the local population and the vehicles crossing these areas.

The final step of all these analytic procedures constitutes the overlay of all these thematic maps through map algebra process allowing the multi-criteria analysis and evaluation of forest fire hazard to the study area. The integration of all inputs was conducted through the following weighted equation, based on the above analysis:

Risk Map ($pixel_{i_{\text{ζ}}}$) = (Land cover * 5) + (Elevation * 1) + (Slope * 2) + (Aspect * 3) + (NDVI * 2) + (NDMI * 3) + (Proximity to road network * 2) + (Proximity to inhabited areas * 1)

Finally, the same process was followed for the development of fire risk map for the year of 1996, using the respective past geodatabases (land cover, road network and vegetation indices – NDVI and NDMI). We considered that the topography factor presented no any change in this timeframe. On the other hand, we adopted as dynamic factors (even though some of them might be not purely dynamic) the land cover, the road network and the vegetation indices, because we examine the impact of these factors in the long run, so even minor changes are expected to affect the total fire risk. Hence, we estimated the per cent change of fire risk from 1996 to 2016 as well as the spatial pattern of these changes (change of risk level per pixel, if any).

3.3.2 Visibility analysis

After creating the final fire risk map, our model is focused on the establishment of a certain number of watchtowers that will largely increase the synergistic action of this preventative measure with the

[3] This weighting process is similar to *Roberto Barbosa et al.* (2010) and *Sharma et al.* (2012), adapted to the local conditions of the island.

above fire risk map. Hence, our goal is to locate watchtowers in positions that will cover a significant percentage of the most susceptible areas (very high and extremely high fire risk); in higher levels of elevation, so that we minimize the slope effect that hinders the visibility; and in areas close to road network, so that this location to be easily accessible by the fire agency personnel. Due to the absence of any past relative information, we tried to maximize the visibility effectiveness (through viewshed analysis) based on a certain number of appropriate locations. The analytical tool that was used for this operation was the visibility tool which is integrated into the ArcGIS toolbox.

First of all, it should be highlighted that there is a shortage of visibility analysis applications for forest fires prevention. This fact is confirmed by the literature review section preceded. One main reason might be related with the difficulties arisen when we face quite variable surface (intense topography). When we face such situations, we might need an enormous amount of financial resources in order to efficiently cover the entire study area in terms of visibility. That means a significant number of lookout towers accompanied with the respective economic cost.

In our case, the study domain constitutes a small island with abrupt surface. However, the size of the study area allows us to apply visibility analysis pursuing the best possible environmental protection (in terms of fire prevention) with the least number of watchtowers.

As previously emphasized, there are very few studies forming a concrete framework on how to effectively apply visibility analysis (Bao et al., 2015; Eugenio et al., 2016). To this end, we tried to establish some logical criteria aiming to the integrated environmental protection as well as to the minimization of the financial cost.

Following, we established the most appropriate criteria that may be used in fire prevention and visibility analysis, such as: i) fire risk potential; ii) elevation; iii) slope; iv) land use appropriateness; and v) proximity to road network. The reasoning for selecting the above criteria was based on some critical aspects such as: i) most importantly, we should ideally locate some watchtowers on the most susceptible areas, a piece of information that is given from the fire risk map; ii) usually, the higher the elevation the better visibility; iii) the slope factor is related with the construction of watchtowers, so, the steeper the slope the more difficult for the construction and visibility of these structures; iv) the land use suitability is clearly related with the appropriateness of the receptors for such purposes. Hence, we avoid water bodies or hostile surfaces (rocky surfaces, current buildings etc.); v) the proximity to road network is related with the accessibility of fire personnel. Elevation, land use suitability and road network proximity constitute the factors that were taken into consideration by a similar study as well (Eugenio et al., 2016). However, the other critical parameters were totally ignored. Even though we should protect any flammable fuel, we should provide a priority to the most vulnerable areas as determined from the respective fire risk map. To this end, we weighted the fire risk factor twice as any other dimension. The following table (Table 3.13) shows the weighting process of these criteria. Nevertheless, it should be stressed that the weights are indicative and subject to changes based on the local conditions. We decided to give a scalable degree of appropriateness of

each factor in order to establish the best possible locations (avoiding the simple intersection of some suitable areas).

Fire risk levels	Visibility weight	Elevation	Visibility weight	Slope	Visibility weight
39 - 88	1	0 - 100	2	0 - 5	10
88 - 100	3	100 - 200	4	5 - 10	9
100 - 110	5	200 - 300	6	10 - 15	7
110 - 121	7	300 - 400	8	15 - 20	5
121 - 134	9	> 400	9	20 -25	3
134 - 169	10			25 - 30	1
Land use appropriateness	**Visibility weight**	**Proximity to road network**	**Visibility weight**		
Artificial structures	0	0 - 100	10		
Purely agriculture	2	101 - 200	9		
Mixture of agriculture and natural vegetation	3	201 - 300	7		
Forested areas	6	301 - 400	5		
		401 - 500	3		
		501 - 600	1		

Table 3.13. Appropriate criteria for the location of candidate watchtowers

Finally, the cumulative result of all these factors is summarized through the following equation:

Most appropriate locations (regions) = Fire risk * 2 + Elevation + Slope + Land use appropriateness + Proximity to road network

After the determination of the most suitable locations for the establishment of watchtowers, a comparative assessment of visibility potential (through viewshed analysis) was conducted among a certain number of candidate positions. Finally, an appropriate combination of minimum watchtowers and maximum visibility (under these specific circumstances) was selected under a cost-benefit framework.

Based on the above methodology framework, the next chapter describes the results of fire risk modelling and visibility analysis. The following graphs (Graph 3.4 and 3.5) summarize the most critical procedures taken place, avoiding including typical geoprocessing processes (dissolve, clip, project etc.), otherwise it would be quite unreadable due to plenty of relative processes conducted for our project.

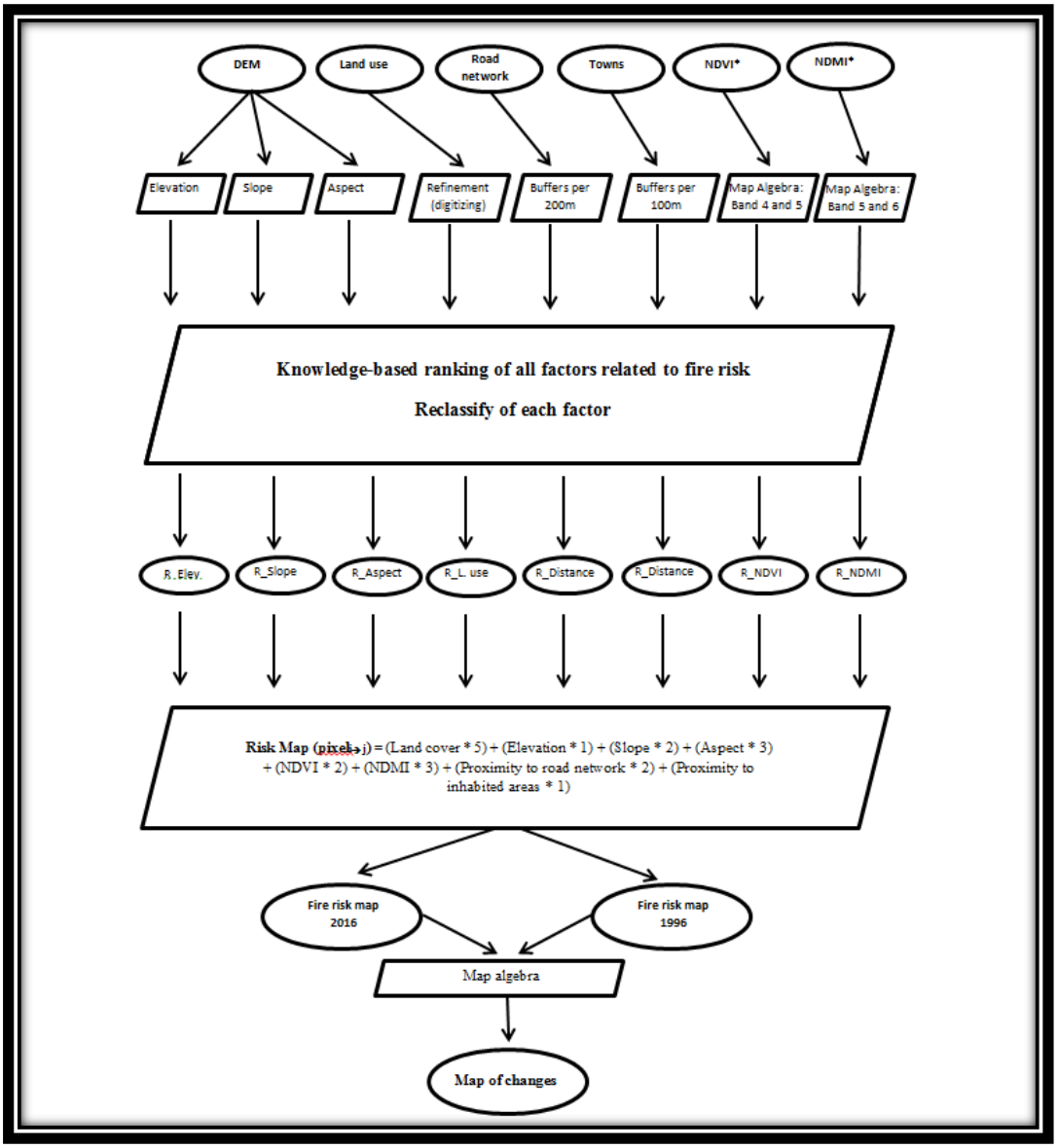

Graph 3.4. Flowchart of fire risk modeling (1996 - 2016)

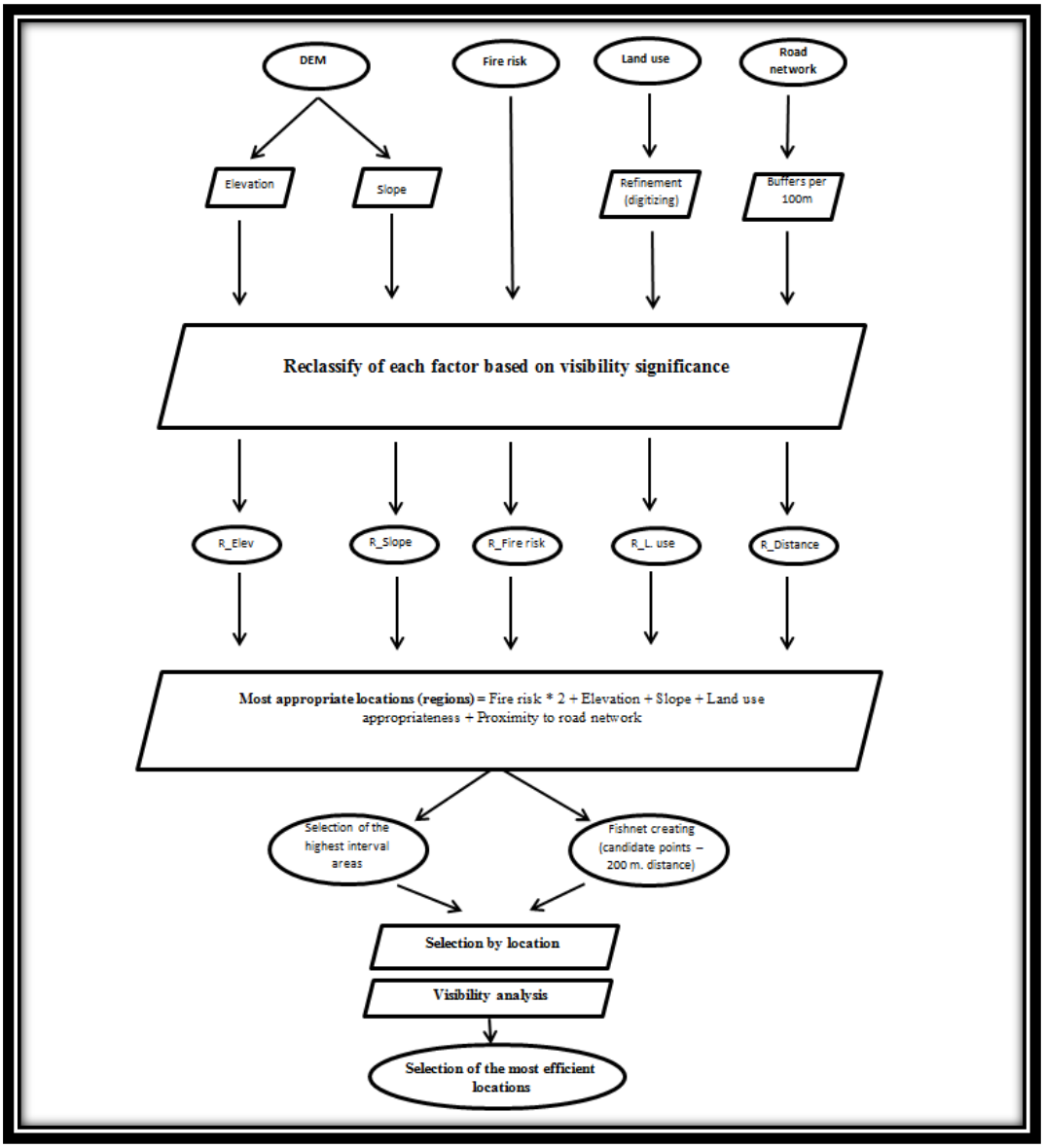

Graph 3.5. Flowchart of visibility analysis

4. RESULTS AND DISCUSSION

This chapter summarizes all the processes described in the methodology section. Specifically, the interaction of each individual factor with forest fire risk is analyzed and discussed for both reference years. Next, a spatiotemporal analysis of fire risk evolution is conducted in order to determine the principal causes that might have led to these changes. Hence, a number of counterbalancing measures is proposed. Finally, based on the previous fire risk modeling, a location scheme of watchtowers is suggested in order to efficiently protect the most vulnerable areas.

4.1 Fire risk modelling

4.1.1 Interrelation of fire risk and key factors - 2016

Firstly, we examined the interrelation of fire risk with topography. The first dimension constitutes the different elevation levels. Elevation is directly related with the type of fire ignition, namely, natural, or human-caused fire events.

In Greece, half of the total fire ignitions (47%) have occurred in the zone from 0 to 300 meters. Hence, we can recognize the significance of this interrelation due to increased number of activities taken place there. However, the most intense fire events have happened in higher altitudes, most probably because these events were become discernible only when they took large dimensions (Tsagari et al., 2011). Here, due to the small size of the island, we determined only four fire zones based on the elevation factor. The following map (Figure 4.1) presents the spatial arrangement of these zones across the island.

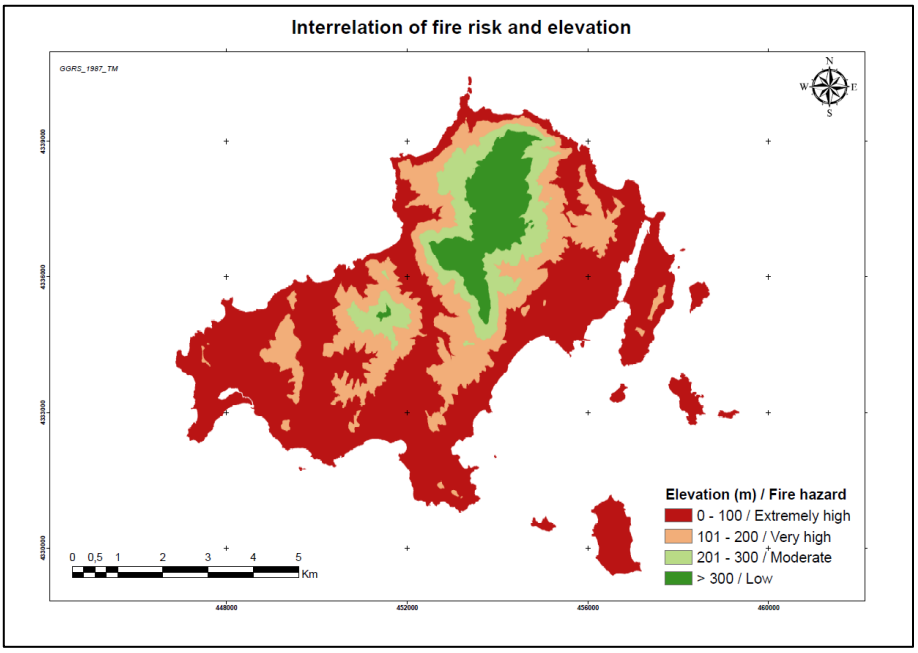

Figure 4.1. Interrelation of fire risk and altitude

Specifically, based on the Table 4.1, we observe that almost 82% of the island belongs to extremely and very high risk (59% and 23% respectively), which means the zone up to 200 meters altitude. The remaining 18% belongs to higher elevation zones (> 200 m.) and lower fire risk. Relied on the results of the above map, we see that the flat and coastal areas primarily cover the perimeter of the study domain, while the higher zones can be found on the north (and interior) part of the island.

Elevation (m.)	Weight	Area (ha)	%	Fire hazard
> 300	2	410	8,4%	Low
201 - 300	5	484	9,9%	Moderate
101 - 200	8	1.122	23,0%	Very high
0 - 100	10	2.872	58,8%	Extremely high
Total	**-**	**4.888**	**100,0%**	**-**

Table 4.1. Area per elevation zone and the respective fire risk

Next, we examined the interaction of fire risk with the slope factor. As we may see from the respective map (Figure 4.2), higher slope is totally related to high fire risk. These areas can be found on the north and interior part of the study area following the pattern of elevation dimension. However, some parts crossing the inner part are characterized from low slope levels which can negatively affect (decreasing) the fire spread and propagation.

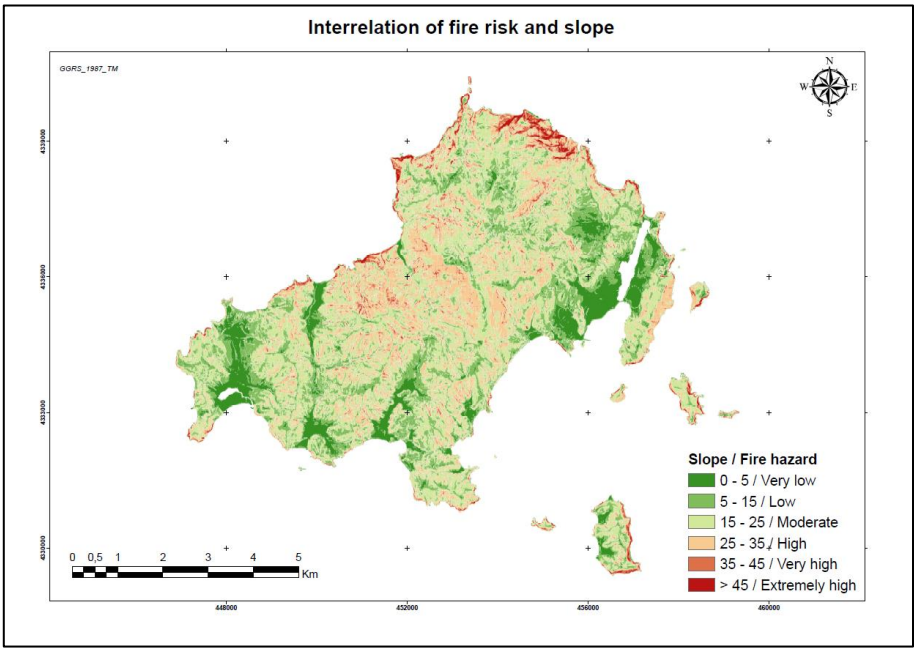

Figure 4.2. Interrelation of fire risk and slope

Statistically, about 29% of the island is of high, very high and extremely high fire risk, while 35% of the study area is characterized by very low and low fire risk (mainly coastal regions). 1/3 of the island belongs to moderate fire risk, as described in the following table (Table 4.2).

Slope	Weight	Area (ha)	%	Fire hazard
0 - 5	1	567	11,6%	Very low
5 - 10	3	1.162	23,8%	Low
15 - 25	5	1.746	35,7%	Moderate
25 - 35	7	1.090	22,3%	High
35 - 45	9	248	5,1%	Very high
> 45	10	75	1,5%	Extremely high
Total	**-**	**4.888**	**100,0%**	-

Table 4.2. Area per slope level and the respective fire risk

Concerning the aspect factor (Figure 4.3), the fire risk zones are more equally distributed along the island in comparison with the other dimensions, as it is presented on the corresponding map.

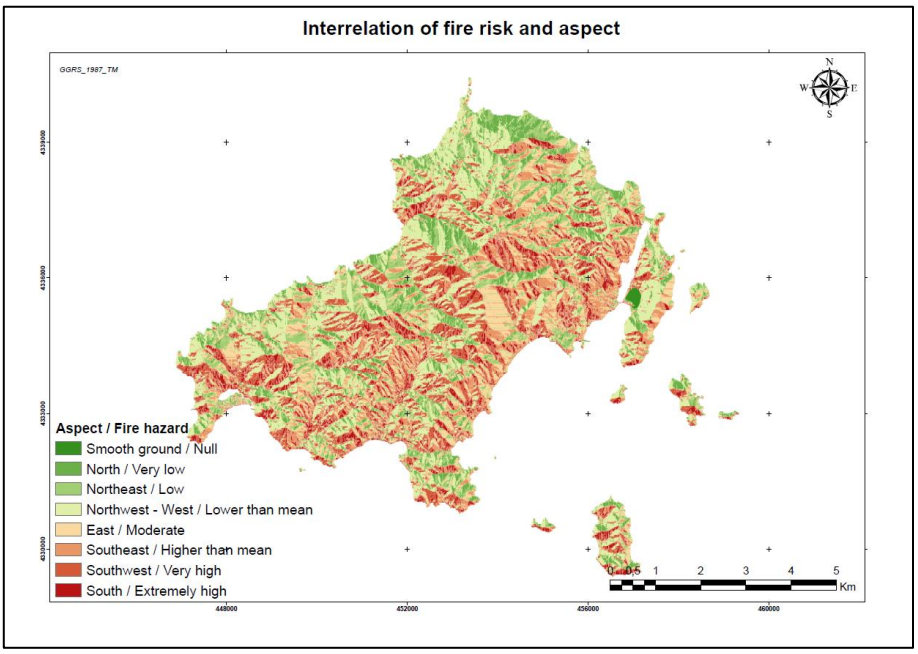

Figure 4.3. Interrelation of fire risk and aspect

Specifically, the areas of very high and extremely high fire risk represent 25% of the total area; the region of high risk covers 13% of the island; the territory of moderate risk covers almost 40%; while the areas of very low and low fire risk represent about 22% of the study domain (Figure 4.3).

Aspect	Weight	Area (ha)	%	Fire hazard
Smooth ground	1	10	0,2%	Null
North	2	494	10,1%	Very low
Northeast	3	558	11,4%	Low
Northwest / West	4	1.279	26,2%	Lower than mean
East	5	683	14,0%	Moderate
Southeast	6	637	13,0%	Higher than mean
Southwest	8	670	13,7%	Very high
South	10	557	11,4%	Extremely high

Total	**-**	**4.888**	**100,0%**	**-**

Table 4.3. Area per aspect level and the respective fire risk

The most critical factor in fire risk modeling constitutes the land cover which is the most closely related information to fuels. That is why, this factor will be assigned with the highest specific weight. Based on the spatial pattern of the land covers, we observe that the most affected type (transitional woodland-shrubs and sclerophyllous vegetation) is mainly located on the southwestern and northern part of the study domain. It should be highlighted that the part of shrubs which can be found on the southwestern region of the island should be considered the most critical, since it is in immediate contact with dense coniferous forests, a fact which may trigger events of very high intensity. The different types of forests are primarily located on the western territory of the study area (except the broadleaved forests which thrive on the northern part), while agricultural land can be found on the coastal areas and on the north of the main town of the island (on the eastern part of the study area). The following map (Figure 4.4) depicts the scalable degree of risk relied on the susceptibility of each land cover type, as described in the methodology section.

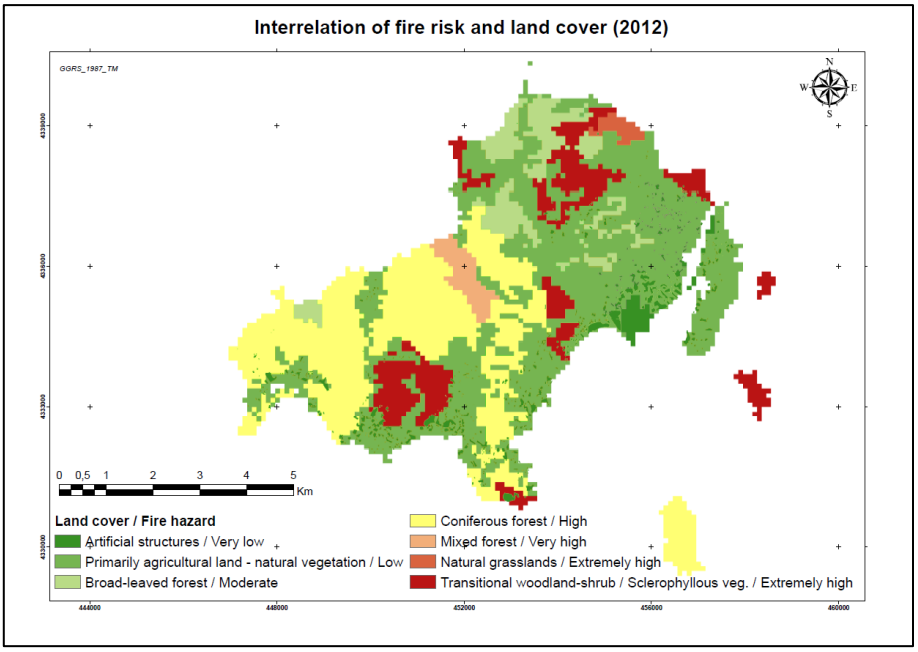

Figure 4.4. Interrelation of fire risk and land cover

The Table 4.4 shows the interrelation of each land cover type and the corresponding fire hazard. We see that the artificial structures themselves are characterized by very low fire hazard due to the nature of the structures; the agricultural fields and sparsely vegetated areas are of low risk and they cover 43% of the island; the broad-leaved forests which are considered of moderate risk cover 8% of the study domain; coniferous and mixed forests are of high and very high risk and cover 32%; while transitional woodland-shrub and sclerophyllous vegetation constitute the most affected land cover types and cover 12% of the entire island. So, one third of the study area is characterized by high, very high and extremely high fire risk based on the nature of fuels.

Land Cover	Weight	Area (ha)	%	Fire hazard
Artificial structures	1	214	5%	Very low
Primarily agricultural land - natural vegetation	3	2.026	43%	Low
Broad-leaved forest	5	362	8%	Moderate
Coniferous forest	7	1.435	30%	High
Mixed forest	8	103	2%	Very high
Natural grasslands	9	43	1%	Very high
Transitional woodland-shrub / Sclerophyllous vegetation	10	566	12%	Extremely high
Total	**-**	**4.749**	**100%**	**-**

Table 4.4. Area per land cover type and the respective fire risk

Next, we examined the interrelation of the NDVI index and the respective fire risk (Figure 4.5). As previously mentioned, NDVI determines the vegetation conditions (healthy/dead fuels, greenness etc.). Based on the analysis preceded, the classification of this index incorporated three distinct intervals. The first one consists of non-vegetated areas (sandy surface, water bodies, rocks etc.) which are characterized by zero fire risk; the intermediate interval mainly includes agricultural territory and possibly parts of shrubs and natural grasslands (for this reason, we assigned a moderate fire risk due to the mixture of these land cover types). Finally, the last interval indicates all types of forest with high degree of density. Consequently, these regions are characterized by high fire risk, because if a fire breaks out on these territories, it might lead to extreme fire events (of very high intensity).

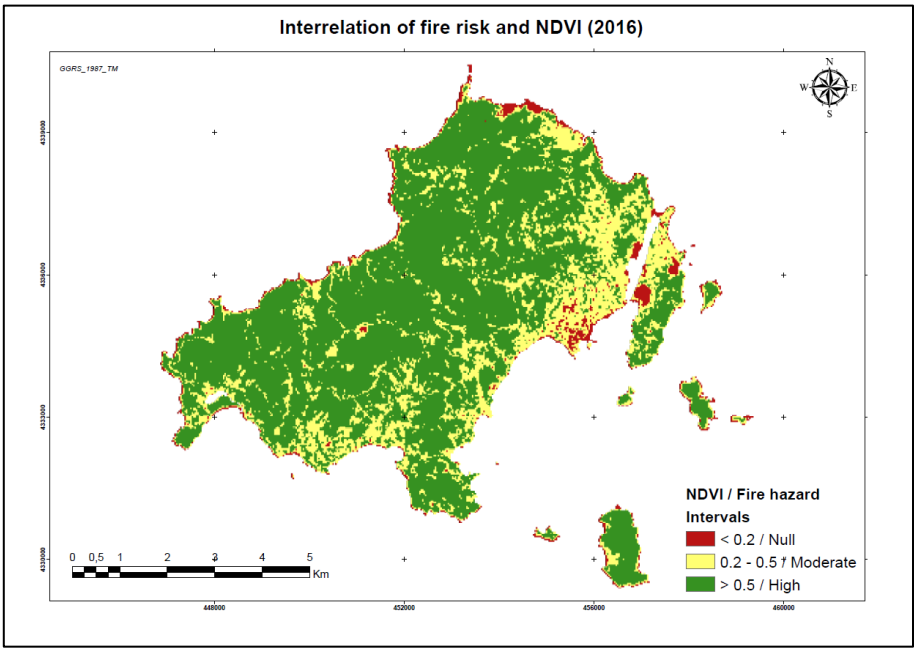

Figure 4.5. Interrelation of fire risk and NDVI

Table 4.5 highlights the fact that the greatest part of the island (72%) is covered by flammable fuels (including all types of forests, shrubs etc.), followed by a considerable amount of agricultural regions

(25%) with moderate fire risk and only 4% of the study domain is covered by totally non-flammable fuels.

NDVI	Weight	Area (ha)	%	Fire hazard
< 0,2	0	177	4%	Null
0,2 – 0,5	5	1.205	25%	Moderate
> 0,5	7	3.507	72%	High
Total	**-**	**4.889**	**100%**	**-**

Table 4.5. Area per NDVI interval and the respective fire risk

Another remote sensing vegetation index constitutes the NDMI which outlines the levels of moisture on vegetated and other types of surface. This critical index may heavily affect the fire spread and propagation. Territories with high degree of moisture concentrate lower possibilities for extreme fire events, while regions with low degree of humidity (and the appropriate combination of forest fuels, e.g. coniferous forests, shrubs etc.) may lead to extensive events of high intensity. The intervals of this index describe the direct interrelation with fire risk. The first two intervals depict the regions with very high and high levels of humidity and primarily consist of forested areas. On the other hand the last two intervals present these regions with low and very low degrees of moisture and significant possibilities for fire ignition and propagation. These territories mainly incorporate the artificial structures and the neighboring land covers (agricultural fields) as well as the transitional woodland-shrubs and the natural grasslands (dead grass), which especially in August (the driest month), are characterized by very low humidity and increased chances for fire ignition. Figure 4.6 presents the spatial pattern of this interrelation.

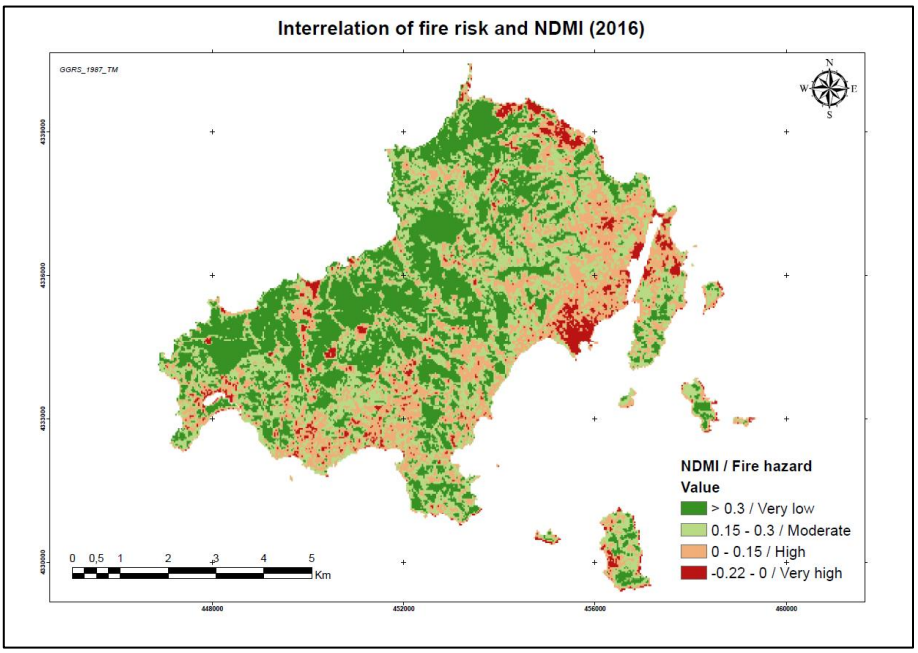

Figure 4.6. Interrelation of fire risk and NDMI

Based on the statistics of this index and the respective fire risk (Table 4.6), we observe that the different types of forest are characterized by higher humidity and lower fire risk, while shrubs, grass and agricultural fields yield to almost 30% of the highest fire risk in terms of moisture.

NDMI	Weight	Area (ha)	%	Fire hazard
> 0,3	1	1.740	36%	Very low
0,15 – 0,3	4	1.714	35%	Moderate
0 – 0,15	7	1.193	24%	High
< 0	9	241	5%	Very high
Total	**-**	**4.889**	**100%**	**-**

Table 4.6. Area per NDMI interval and the respective fire risk

Concerning, the impact of anthropogenic dimension, we firstly examined the proximity to road network, since accessibility constitutes a key factor to accidents, arsons and other potential causes for the ignition of a forest fire event. In order to determine these conceivable zones, we created distinct zones indicating the possibilities of a fire ignition. Each zone has a width of a 100 meters up to 500 meters (with scalable degree of fire risk), given the total size of the island. As can see from the respective map (Figure 4.7), the most dangerous zone (0-100 m.) covers a significant part of the study area, a fact that reflects the dense road network compared to the area of the island.

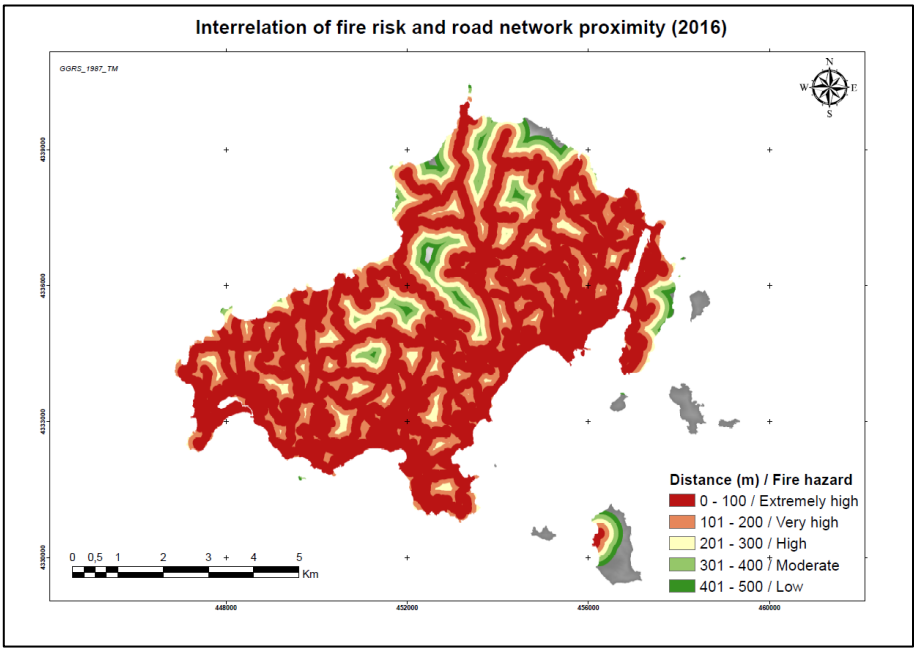

Figure 4.7. Interrelation of fire risk and road network proximity

The above conclusions are confirmed by the following table (Table 4.7) which presents the total area per zone. Based on this table, we see that 83% of the island lies under very high and extremely high risk; 12% of the study domain is characterized as moderate and high risk; and only 5% lies under low or not at all risk. As previously emphasized, this fact is due to extended and very dense road network covering the entire island.

Proximity to road network (m)	Weight	Area (ha)	%	Fire hazard
> 500	0	169	3%	None
401 - 500	2	78	2%	Low
301 - 400	5	196	4%	Moderate
201 - 300	7	415	8%	High
101 - 200	8	1.112	23%	Very high
0 - 100	10	2.917	60%	Extremely high
Total		**4.888**	**100%**	

Table 4.7. Area per road network buffer zone and the respective fire risk

Last factor of the modeling is the impact of artificial structures' proximity which includes the main town of the island and many individual structures (dwellings; telecommunications structures etc.). Certainly, the Corine Land Cover is coming on coarse scale and capturing only the extended urban area (due to the minimum mapping unit). However, the extended existence of many structures inside the island may seriously increase the fire ignition possibilities. To this end, using aerial imagery of high spatial resolution (orthophotos), we digitized these individual entities and created the proximity zones every 200 meters which is a small walking distance. Map 4.8 shows the spatial pattern of this interrelation emphasizing the extended –not adequately organized- urbanization on the coastal areas as well as in the interior of the island next to forested territories. The most organized receptor lies on the eastern part of the island where the main town with all the necessary services is located. Finally, it should be noted that the majority of these structures are located near to agricultural fields, shrubs and natural grasslands, where the construction of buildings is easier and the dependency is higher.

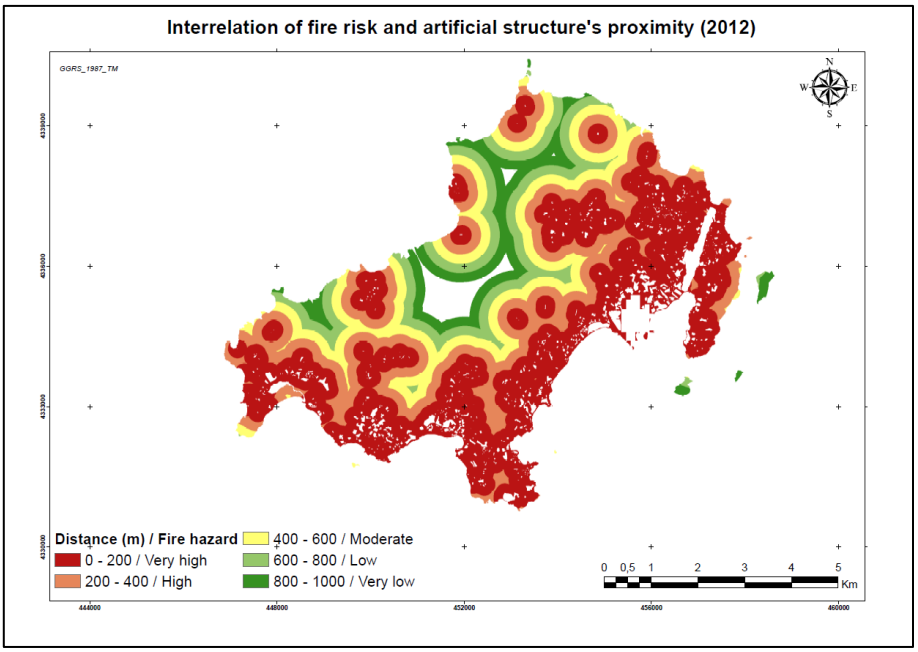

Figure 4.8. Interrelation of fire risk and artificial structure's proximity

The Table 4.8 reflects the interrelation of different levels of proximity with the corresponding fire risk. Here, it should be mentioned that we avoided assigning the highest fire risk due to the fact that

even though the first zone concentrates the highest possibilities for fire ignition, a fire event may be discernible from the theoretically many viewers (local inhabitants) and the moving vehicles across the road network. For this reason, this factor will receive the lowest specific weight in the general categories which affect the fire risk levels. Statistically, we see that the first 400 meters nearby artificial structures are characterized of 61% of high and very high risk, while the remaining 39% can be considered of low (26%) and moderate fire risk (13%).

Proximity to artificial structures (m)	Weight	Area (ha)	%	Fire hazard
> 1000	0	492	10%	None
800 - 1000	2	327	7%	Very low
600 - 800	3	463	9%	Low
400 - 600	5	638	13%	Moderate
200 - 400	7	959	20%	High
0 - 200	8	2.010	41%	Very high
Total		**4.888**	**100%**	

Table 4.8. Area per artificial structure buffer zone and the respective fire risk

4.1.2 Fire risk modeling – Development of the fire risk map for 2016

Final output of fire risk modeling constitutes the integration of all the contributing weighting factors. The fire risk map was created based on the equation presented in the methodology section.

The following map (Figure 4.9) depicts the spatial pattern of fire risk in the island of Skiathos based on the most recent and updated information. First of all, it should be emphasized that the fire risk scale ranges from 19 (minimum possible) to 190 (maximum possible) as calculated from the respective equation. Hence, we decided to incorporate two distinct scales. The first one is more general and easily understandable for the general public; the second one describes the exact weighted result of fire risk for each pixel.

Concluding, the most susceptible areas are located on the southwestern and western part of the island as well as in few regions in the north. The cumulative impact of the most affected land cover types (shrubs and forests); the high degree of accessibility and proximity to infrastructures and other artificial structures; the low degree of moisture in some specific areas (especially on the south and northeast part of the study area); and the geomorphological characteristics (low elevation; moderate to steep slope and south aspect) yielded to this specific spatial pattern of fire risk. On the other hand, less affected land cover types with lower degree of accessibility and proximity to artificial structures, higher elevation, north aspect and moderate to higher degree of humidity present totally different spatial structure. This case is reflected for the broadleaved forests on the north of the island. The same pattern applies to the least affected land cover types (agricultural fields, urban areas) due to the nature of this fuel (quite less flammable), even though other factors may heavily affect the fire risk (accessibility, proximity to inhabited areas; low elevation; south aspect and lower degree of moisture).

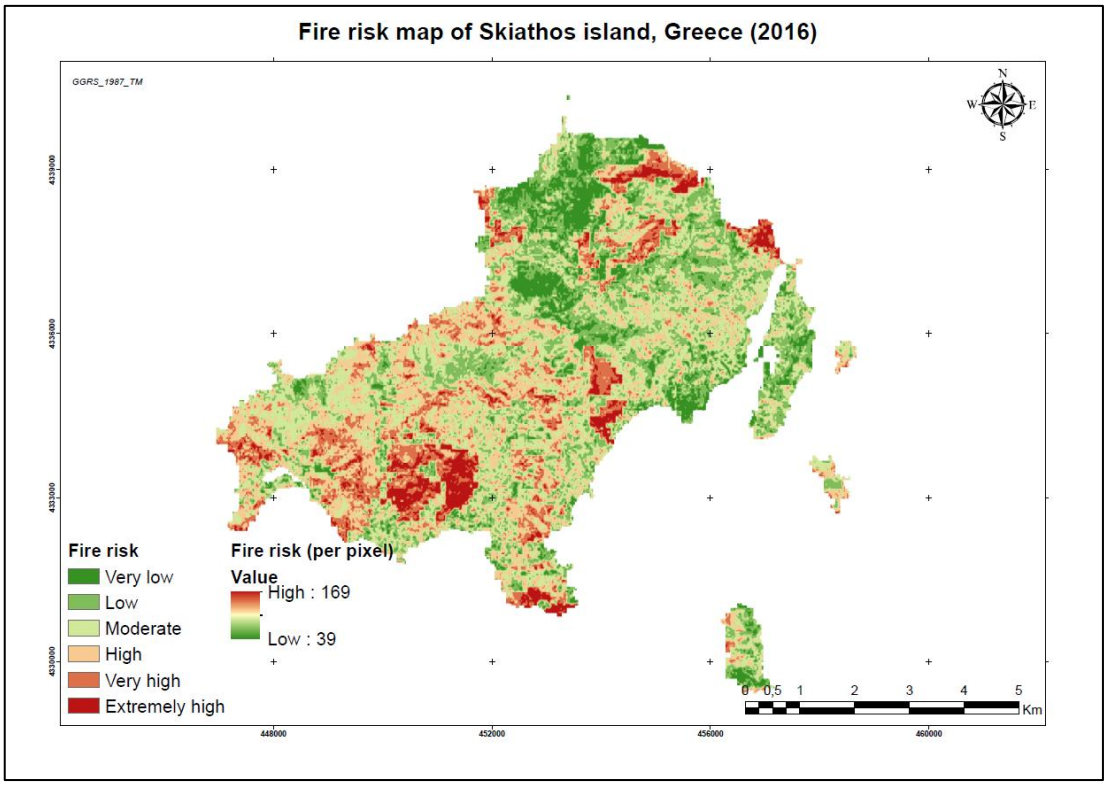

Figure 4.9. Fire risk for the island of Skiathos (2016)

The overall statistics of the fire risk map indicate that 34% of the entire study area is covered by territory of low fire risk; 27% of moderate risk; 34% of high and very high risk, while there is a 6% of the island which is characterized of extremely fire risk. The Table 4.9 summarizes the previous conclusions.

Fire risk levels	Area (ha)	%	Fire hazard
39 - 88	508	11%	Very low
88 - 100	1.055	23%	Low
100 - 110	1.264	27%	Moderate
110 - 121	988	21%	High
121 - 134	587	13%	Very high
134 - 169	285	6%	Extremely high
Total	**4.686**	**100%**	

Table 4.9. Area per fire risk level

4.1.3 Interrelation of fire risk and key factors – 1990/1996

In order to study the spatiotemporal evolution of fire risk in a timeframe of 20 years approximately, we had to adopt the same reasoning and weighting process. Firstly, it should be stressed that we examined this evolution based on the contribution of dynamic factors (in the long run), namely, the changes in land cover/uses; the proximity to road network (because new segments of roads might have been constructed and others might have been eliminated); the proximity to artificial structures (new structures might have constructed within this timeframe); and the vegetation indices which describe

the greenness, the conditions and the moisture of vegetation. These last indices are directly related with the climate fluctuations through time.

The following map (Figure 4.10) depicts the spatial arrangement of land cover/use in 1996, enriched with the specific individual structures (while they are not visible on coarse scale maps), as digitized from the corresponding orthophotos.

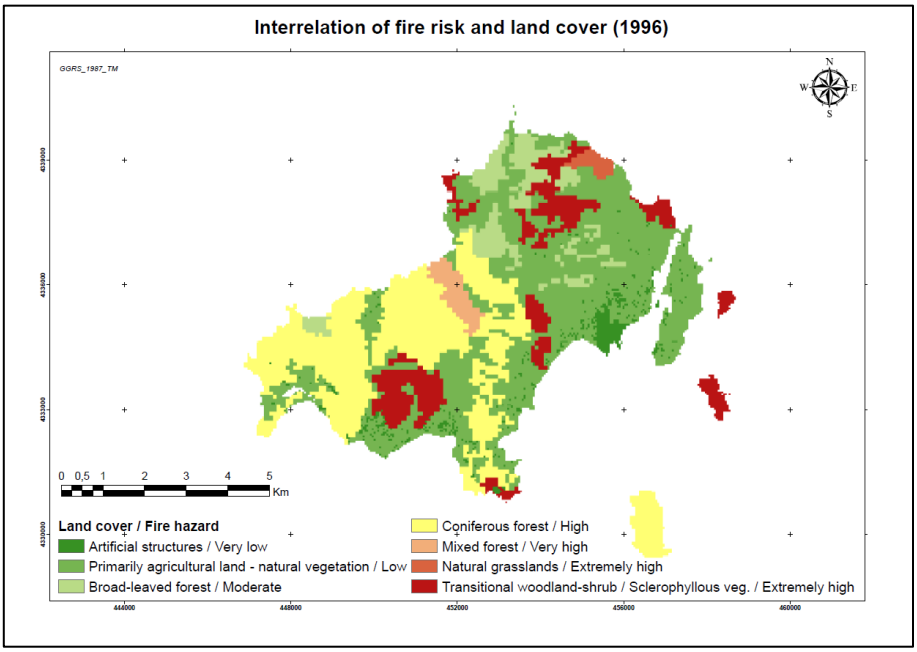

Figure 4.10. Interrelation of fire risk and land cover (1996)

The Table 4.10 presents the interrelation of each land cover type with the respective fire risk. We may see that no significant changes have occurred in land cover/uses within this period due to the nature of the study area (a small island).

Land Cover	Weight	Area (ha)	%	Fire hazard
Artificial structures	1	148	3%	Very low
Primarily agricultural land - natural vegetation	3	2.112	44%	Low
Broad-leaved forest	5	366	8%	Moderate
Coniferous forest	7	1.433	30%	High
Mixed forest	8	100	2%	Very high
Natural grasslands	9	45	1%	Extremely high
Transitional woodland-shrub / Sclerophyllous veg.	10	571	12%	Extremely high
Total		**4.774**	**100%**	

Table 4.10. Area per land cover type and the respective fire risk (1996)

We continue with the condition of NDVI in 1990, where a clear image without cloud interference has been retrieved. As we see from the Figure 4.11, there is a significant change between the two reference years, however, some errors in the image might be present, since the majority of the values

lie below 0,5 even though many forested areas exist. It seems that the entire vegetated regions along with agricultural fields are merged into the intermediate interval. However, we consider that the image information is correct in this stage of analysis, since there is no a clear proof the errors.

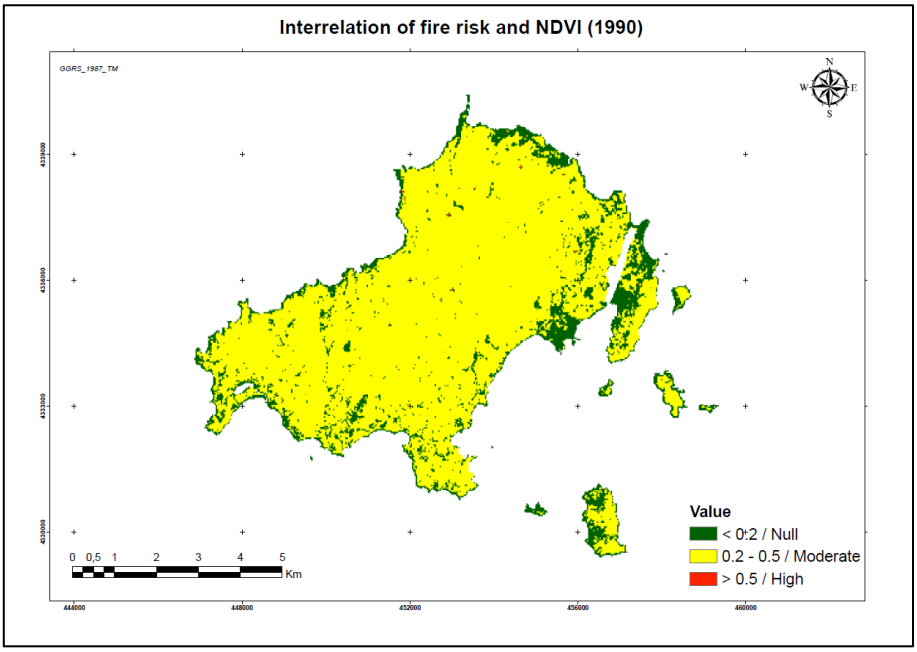

Figure 4.11. Interrelation of fire risk and NDVI (1996)

This fact is confirmed by the Table 4.11 where 85% of the entire study area is covered by the second class.

NDVI	Weight	Area (ha)	%	Fire hazard
< 0.2	0	731	15%	Null
0.2 - 0.5	5	4.155	85%	Moderate
> 0.5	7	3	0%	High
Total		**4.889**	**100%**	

Table 4.11. Area per NDVI interval and the respective fire risk (1996)

The same process was followed for the moisture index. As we may conclude from the Figure 4.12, the least moisture levels can be found on urbanized territories; on agricultural fields and on shrubs. On the contrary, the highest moisture levels were located on the forested areas. This map is quite compatible with the reality.

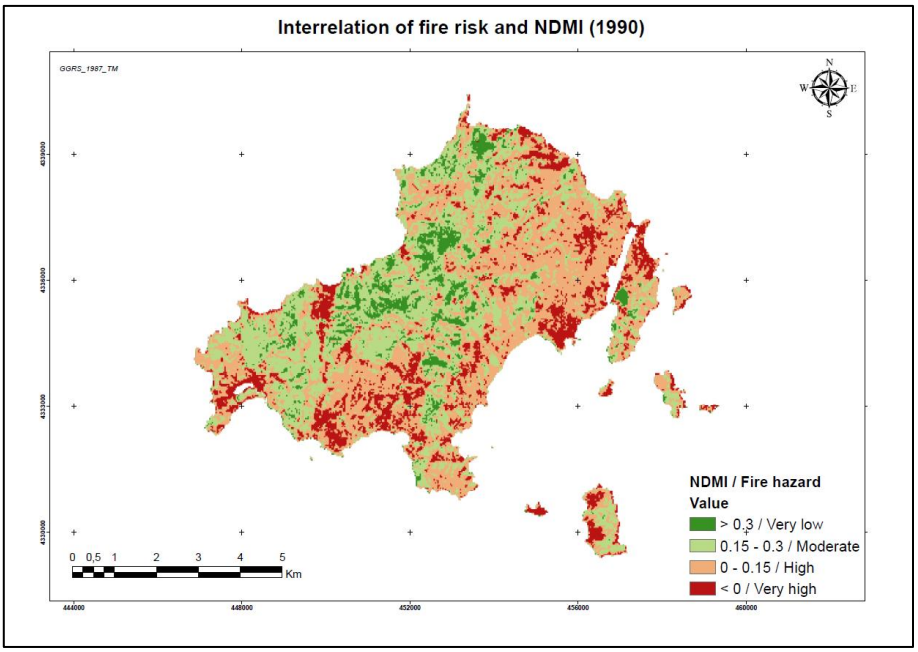

Figure 4.12. Interrelation of fire risk and NDMI (1996)

The next table (Table 4.12) shows the interrelation between the different levels of humidity and the respective fire risk. Indeed, an obvious change occurred between the two years.

NDMI	Weight	Area (ha)	%	Fire hazard
> 0.3	1	362	7%	Very low
0.15 - 0.3	4	1.668	34%	Moderate
0 - 0.15	7	2.100	43%	High
< 0	9	758	15%	Very high
Total		**4.888**	**100%**	

Table 4.12. Area per NDMI interval and the respective fire risk (1996)

Regarding the human causes, the spatial arrangement of road network and the corresponding percentages in relation to fire risk are presented by the following map (Figure 4.13) and table (Table 4.13). As previously mentioned, the processes of fire risk determination are identical with the processes for 2016.

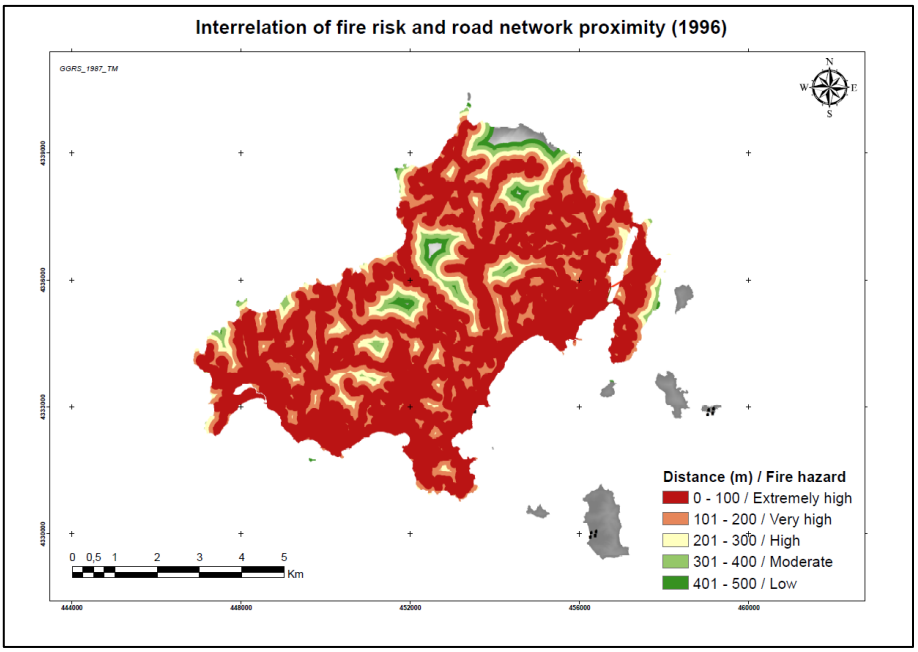

Figure 4.13. Interrelation of fire risk and road network proximity (1996)

As we observe from the Figure 4.13 and Table 4.13, there is a change between the two years of reference, though, it is not so significant.

Proximity to road network (m)	Weight	Area (ha)	%	Fire hazard
> 500	0	154	3%	None
401 - 500	2	65	1%	Low
301 - 400	5	160	3%	Moderate
201 - 300	7	357	7%	High
101 - 200	8	983	21%	Very high
0 - 100	10	3.069	64%	Extremely high
Total		**4.788**	**100%**	

Table 4.13. Area per road network buffer zone and the respective fire risk (1996)

Finally, the last anthropogenic factor is related with the proximity to artificial structures as well. The following map (Figure 4.14) and table (Table 4.14) adopted the same conceivable zones and weighting process as occurred for 2016.

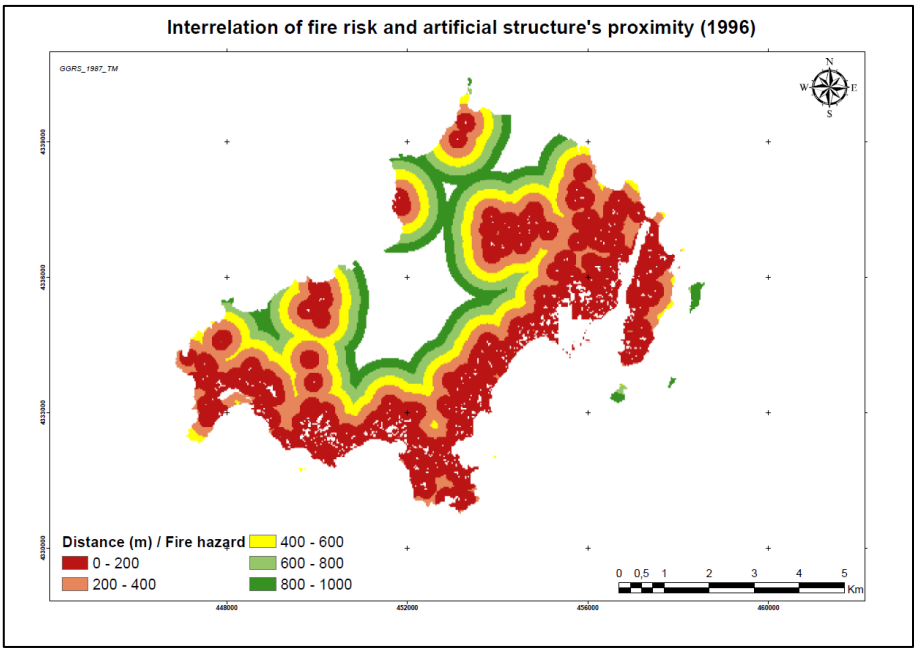

Figure 4.14. Interrelation of fire risk and artificial structure's proximity (1996)

Proximity to artificial structures (m)	Weight	Area (ha)	%	Fire hazard
> 1000	0	854	18%	None
800 - 1000	2	404	8%	Very low
600 - 800	3	454	9%	Low
400 - 600	5	545	11%	Moderate
200 - 400	7	853	18%	High
0 - 200	8	1.733	36%	Very high
Total		**4.843**	**100%**	

Table 4.14. Area per artificial structure buffer zone and the respective fire risk (1996)

As we may conclude, there is indeed a difference between 1996 and 2016, while more dwellings and other artificial structures have been constructed.

4.1.4 Fire risk modeling – Development of the fire risk map for 1996

Final output of fire risk modeling constitutes the integration of all the contributing weighting factors. The fire risk map was created based on the equation presented in the methodology section.

The following map depicts the spatial pattern of fire risk in the island of Skiathos for the reference year of 1996. The scale/intervals of fire risk map are the same with the scale of risk for the most recent year (2016) for comparative reasons.

Similar conclusions with the first fire risk map (Figure 4.15) can be drawn, since no significant changes have been observed, especially on the land cover types and their spatial arrangement. These

slight changes in fire risk evolution are described in the following section. Again, the spatial arrangement of land covers along with the NDMI index seem to lead and form the fire risk map, since these factors concentrate the highest general weight. The remaining factors indeed affect the fire risk but not as the prevalent force. Finally, it should be stressed that the lowest score of the pixel is 49 instead of 39 for 2016. That is a first evidence that the total fire risk might be decreased through time for several reasons.

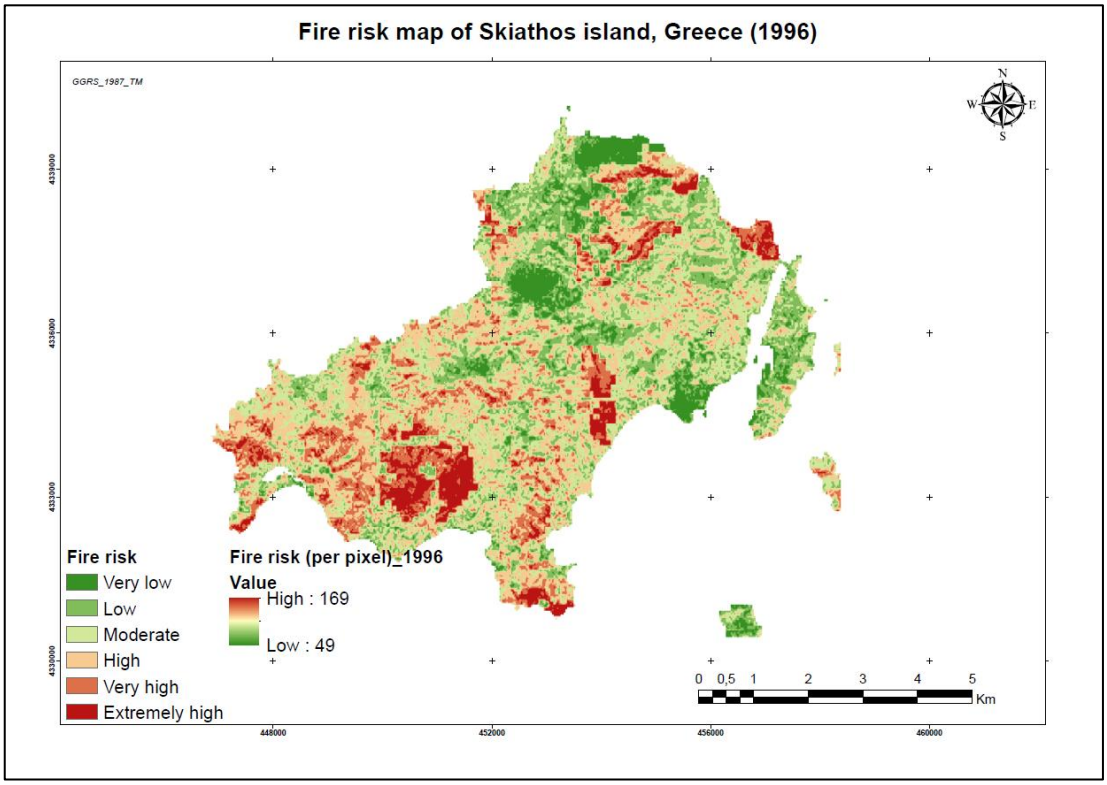

Figure 4.15. Fire risk for the island of Skiathos (1996)

The overall statistics of the fire risk map indicate that 30% of the entire study area is covered by territory of low fire risk; 27% of moderate risk; 36% of high and very high risk, while there is a 7% of the island which is characterized of extremely fire risk. The Table 4.15 summarizes the previous conclusions.

Fire risk levels	Area (ha)	%	Fire hazard
39 - 88	415	9%	Very low
88 - 100	957	21%	Low
100 - 110	1.235	27%	Moderate
110 - 121	1.062	23%	High
121 - 134	625	13%	Very high
134 - 169	342	7%	Extremely high
Total	**4.635**	**100%**	

Table 4.15. Area per fire risk level (1996)

4.1.5 Spatiotemporal evolution of fire risk maps

In this section, we explored the fire risk evolution in Skiathos island from 1996 to 2016. As previously mentioned, there are no significant changes in fire risk, mainly because the land cover change was marginal. In addition, reasonably, this factor concentrates the highest weight and inevitably greatly affects the fire risk. However, we can see these slight changes in two maps. The first one (Figure 4.16) depicts the percentage change of fire risk score within the given time frame. As we can observe from the Figure 4.16, there is a general decrease of fire risk (up to 48,4%) across the entire study area, while there are some specific areas that the fire risk increased more than 95%. However, these regions are very few and can be found in the interior of the island and in some parts in the north.

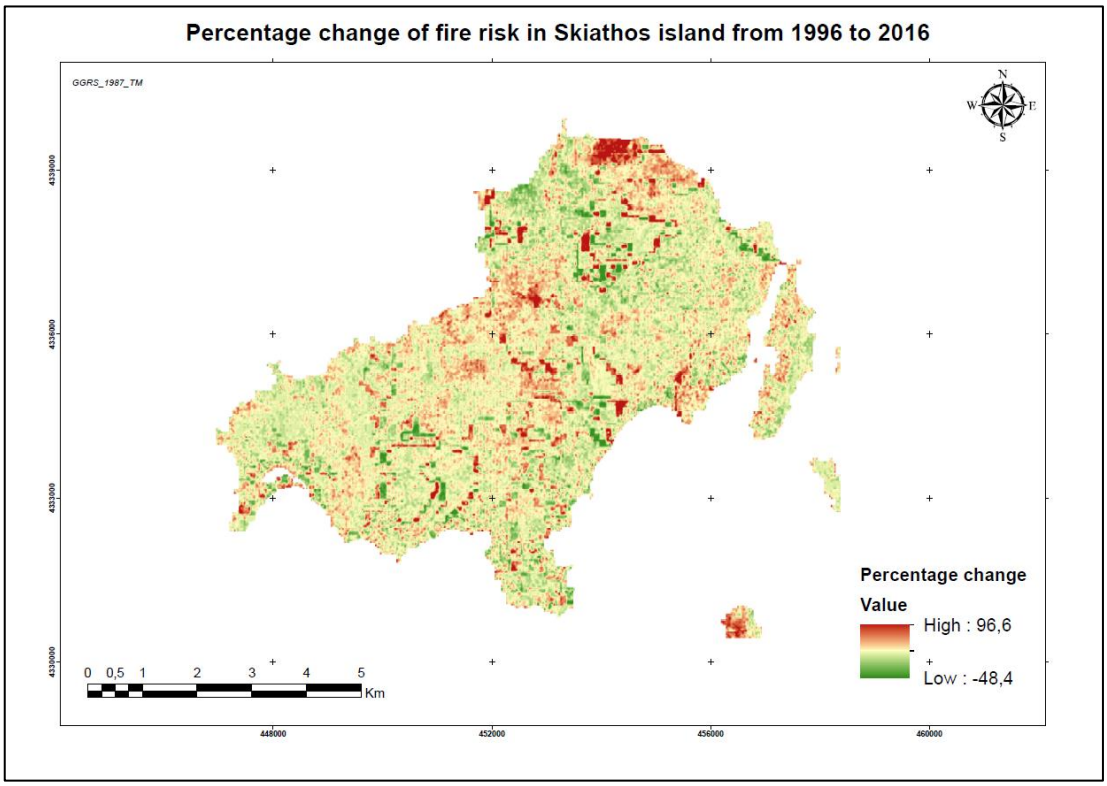

Figure 4.16. Percentage change of fire risk from 1996 to 2016

These slight changes are due to some specific and certain reasons, such as:

1) Most importantly, the land covers changes. In 2016, more artificial structures have been built, a fact that reduced the fuel for burning. The replacement of forest or agricultural fuel with artificial structures plays a critical role in fire risk.

2) The NDMI index. Even though, the satellite images are derived on the same month (August), it seems that there is much more drought in 1996 compared to 2016 in many territories. Probably, 10 days later, the levels of drought increased leading to more severe fire hazard. Hence, we understand the significance and range of this factor even after a few days (on the driest month).

3) Since more artificial structures have been built, a slight increase of fire risk has been occurred due to proximity with these entities. However, the general weight is quite lower than the land cover contribution.

4) The NDVI played a distinct role, since there are very dense and healthy forests in 2016 compared to the high degree of mixture between forests and agricultural fields/shrubs in 1996.

The last map (Figure 4.17) shows the fire risk levels changed between those two years. As we may conclude, most of the territory remained within the same fire risk class, followed by decrease of fire risk level and some hotspots with increase of risk levels.

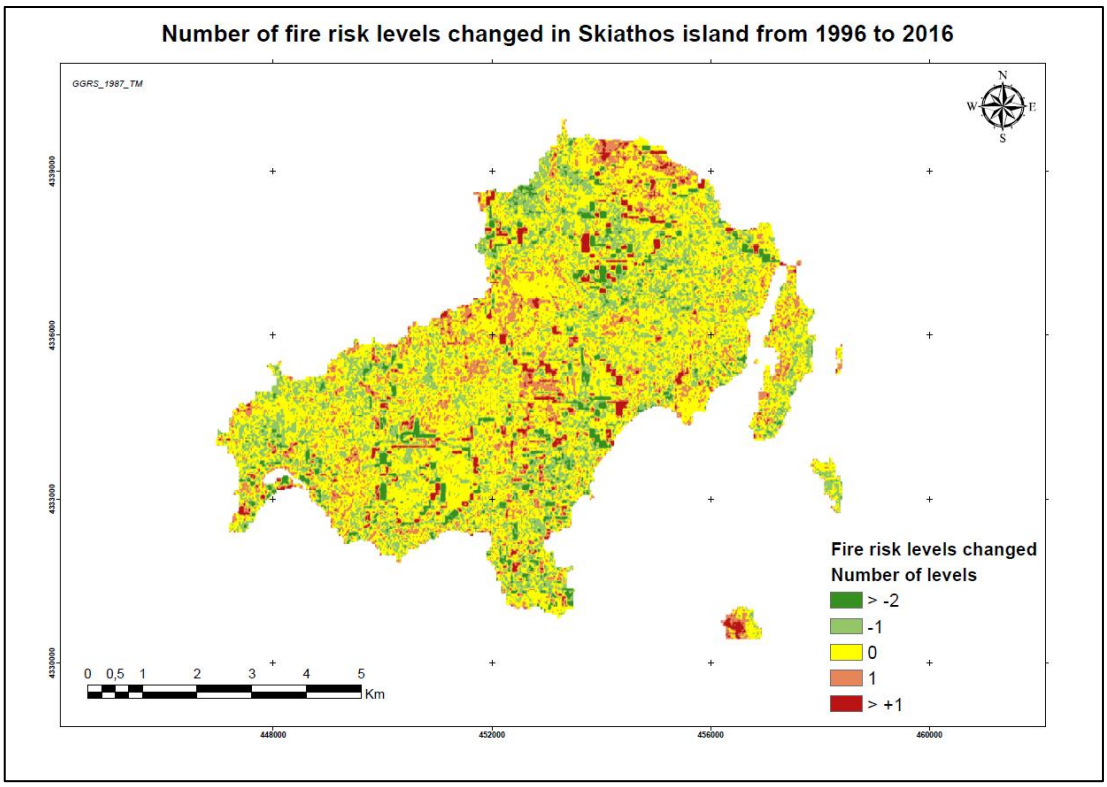

Figure 4.17. Fire risk levels changed from 1996 to 2016

Some good practices to reduce the fire risk especially on the areas where a remarkable (positive) change was noted can include: fuel treatment; recurring monitoring of these susceptible areas for immediate detection of fires through the establishment of watchtowers; utilizing drones and other online platforms with predictive capability of extreme meteorological conditions etc.

4.2 Visibility analysis – Watchtowers establishment as a preventative measure

Before applying visibility analysis, we should find the potential positions for locating the watchtowers. In order to do so, we had to divide the study area equally, so that we can capture any variability in the following criteria. Thus, we applied a fishnet across the entire study area and we selected the mid points of each square of the fishnet (Figure 4.18). The horizontal and vertical distance was set to 200 meters.

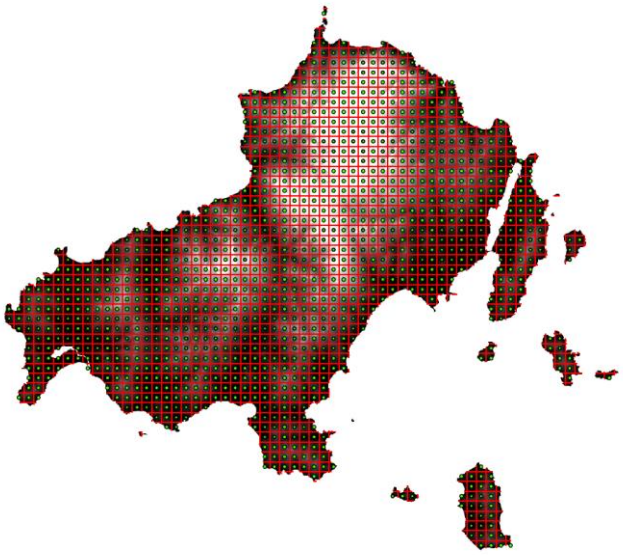

Figure 4.18. Candidate locations across the entire study area (200 meters distance between each other)

The Figure 4.19 presents the most appropriate regions for locating the requested watchtowers, based on methodological framework presented in the methodology section (key factors; weighting process; suitability algorithm etc.).

We see that the best location took the score of 55, while the worst location took a score of 9.

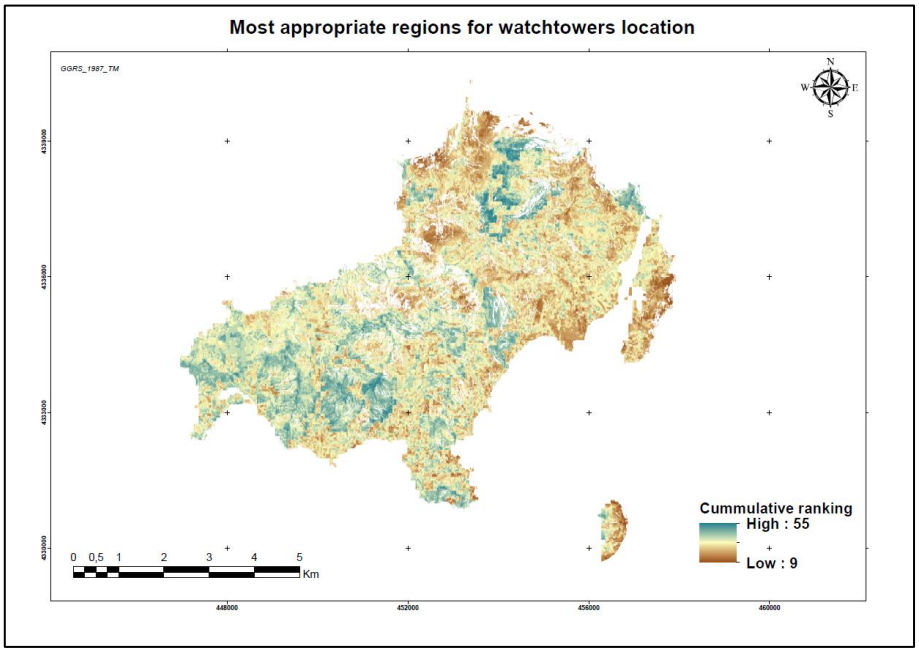

Figure 4.19. Cumulative ranking of suitability for watchtowers location

Consequently, based on the natural breaks intervals, we kept the (last) most efficient interval, ranging from 46 to 55. Afterwards, we selected the appropriate locations (Figure 4.19) that fall into this

specific interval (specific regions from Figure 4.20). Consequently, 29 candidates were found, from which, 14 are located in the north and 15 are located in the south. Due to the fact that there was a big gap in the middle of the island, we considered to take into account two more candidate positions in higher altitudes in the center of the study area.

Next step constituted the visibility analysis for each candidate position. The combination of the Figure 4.20 and Table 4.16 presents the exact location of each watchtower accompanied with the respective visibility potential.

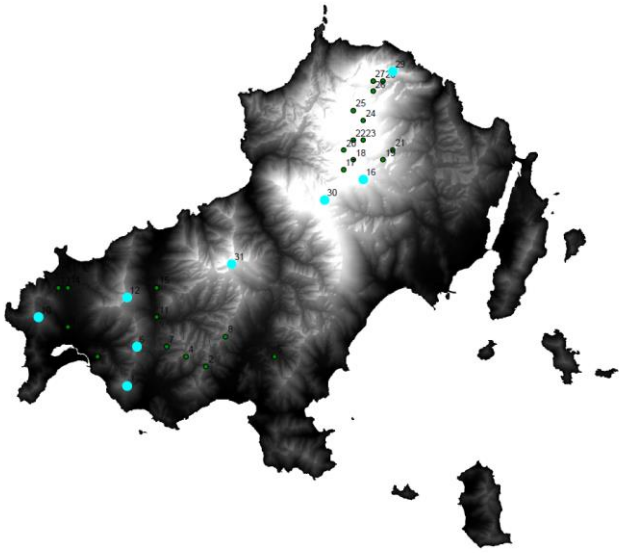

Figure 4.20. Selection of the most appropriate (efficient) locations

No.	Elevation (m)	Visible ha	% of the island		No.	Elevation (m)	Visible ha	% of the island
1	108	399	8%		17	404	114	2%
2	93	253	5%		18	378	16	0%
3	17	64	1%		19	306	50	1%
4	113	182	4%		20	388	146	3%
5	30	99	2%		21	243	9	0%
6	119	419	9%		22	421	108	2%
7	62	89	2%		23	406	63	1%
8	122	295	6%		24	421	36	1%
9	8	150	3%		25	385	16	0%
10	102	378	8%		26	338	18	0%
11	24	52	1%		27	375	181	4%
12	185	558	11%		28	348	299	6%
13	25	205	4%		29	343	377	8%
14	18	106	2%		30	408	738	15%

15	21	57	1%		31	317	584	12%
16	370	374	8%					

Table 4.16. Visibility analysis of the best candidate locations

Based on the Figure 4.20 and Table 4.16, we observe that there is a conceivable line beginning from southwest to northeast part of the island. Another conclusion is that the elevation factor, even though it is important, there are many cases where higher elevation led to very small amount of visibility. So, we should emphasize the impact of geomorphology (slope) that should be taken into account in such projects. In addition, due to this abrupt surface, we see that the mean visibility potential is only 4%. Thus, we chose the most efficient watchtowers with potential from 8 to 15%. Cumulatively, these structures cover 3.829 ha (78% of the total area of the island), however, this percentage is not without overlapping. Even though overlapping is not a negative effect in our phenomenon, a significant amount of overlapping has been observed.

The following map (Figure 4.21) depicts the final selected locations of watchtowers along with their visibility effectiveness (through viewshed analysis among the final selected positions) across the territory of the island.

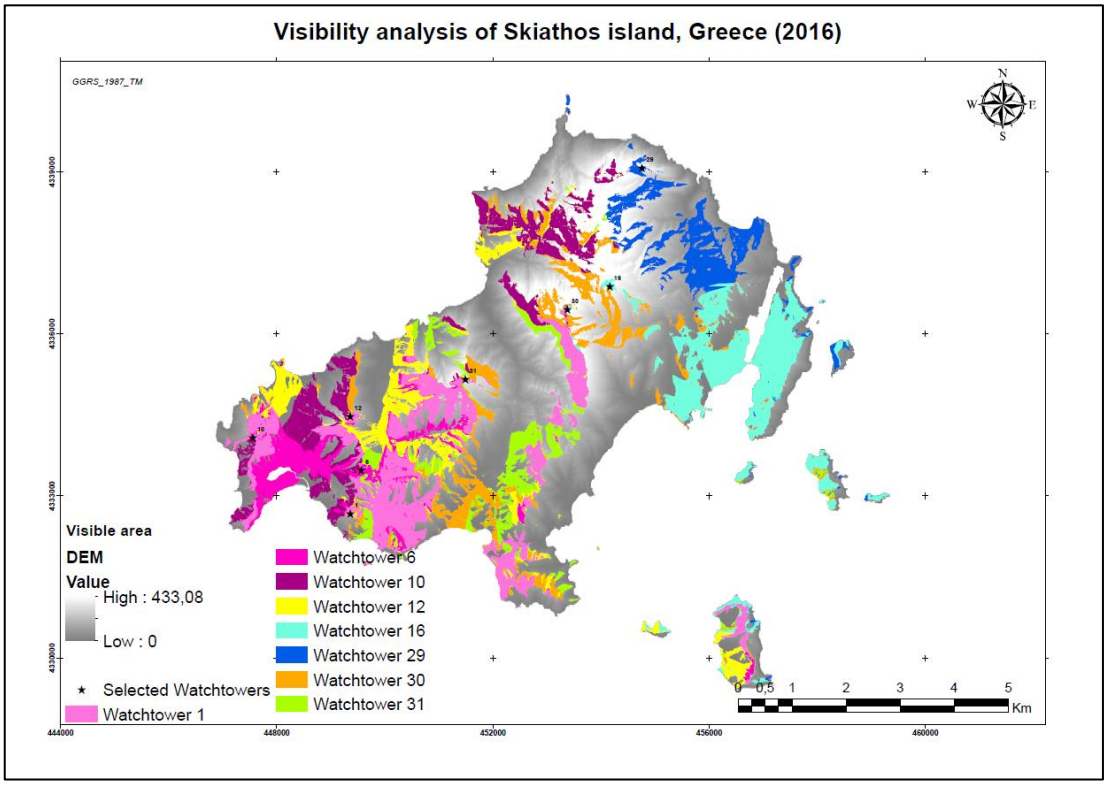

Figure 4.21. Location and visibility of the final selected watchtowers

Relied on this map, we observe that specific regions of the study area are adequately covered, while others remain unmonitored. Specifically, the southwestern and the eastern part of the island fall within the visibility potential of multiple watchtowers. The most important fact here is that even though many of the most susceptible areas are not directly visible from the given points, they are located just

nearby to the visibility radius of the above positions. Here, it should be noted that the geomorphology of the study domain plays a prominent role, since most of the watchtowers may yield to marginal visibility range. This is confirmed by the visibility percentages of the examined 31 locations that met the predefined criteria. Beyond this, we explored the visibility potential of random positions, especially where no visibility is achieved (central areas and areas with the highest elevation in the north), and the result provided quite small percentages.

The next table (Table 4.17) presents the total visible area per fire risk level. We see that more than 40% of the entire island is visible from the location scheme of just 8 watchtowers. The intense topography constituted the most critical barrier in increasing this percentage. In addition, we conclude that the most risky regions are visible almost half of them (close to 45%), except the extremely high risk areas where almost 40% is visibly covered. Here, beyond the obvious reason of topography, the small territory of this category (only 6% of the study domain) was another reason of this small percentage.

Fire risk levels	Area (ha)	%	Fire hazard	Visible area (ha)	% per fire risk level
39 - 88	508	11%	Very low	225	44%
88 - 100	1.055	23%	Low	465	44%
100 - 110	1.264	27%	Moderate	542	43%
110 - 121	988	21%	High	432	44%
121 - 134	587	13%	Very high	250	43%
134 - 169	285	6%	Extremely high	101	36%
Total	**4.686**	**100%**	**-**	**2.015**	**43%**

Table 4.17. Interrelation of visibility potential and fire risk

Finally, it should be highlighted that given the extreme topography of the island, these percentages can be considered satisfying enough, but not optimal. They can be considered satisfying enough in a cost-benefit framework. Otherwise, the establishment of an enormous amount of watchtowers should be demanded, while the added value of each one is quite marginal. This fact includes the demand of very high amount of fiscal resources. Some good practices to counterbalance the relative small percentage of visibility could include; the extensive patrols in unmonitored regions through the intense road network of the island; the adoption of drones covering the aforementioned areas, especially when extreme meteorological conditions are expected.

4.3 Limitations and future perspectives

During the implementation of the project, some limitations and future perspectives have been recognized. Primarily, some technical issues came up especially regarding the historic satellite images. Even though we tried to fix these issues, some problems seemed to be inherent to the images themselves. However, we concluded that they did not affect the final result to a great extent. In addition, due to the small size of the island, there was no any weather station so that we can

interpolate some meteorological indices and developing the respective thematic maps (e.g. temperature, wind effect, precipitation, evapotranspiration etc.). We handled this restriction by using the most suitable remote sensing vegetation index (NDMI) as a proxy of humidity. Another future perspective of the project lies in the weighting process. Specifically, we aim to apply Analytical Hierarchy Process instead of Knowledge-based weighting process, due to the fact that the land cover dimension seemed to heavily affect the fire risk. Indeed, the land cover is leading the fire risk, however, the difference compared to other factors could be a little less stronger. Moreover, programming scripts may help to find the optimal locations of watchtowers (maximization of visible area), saving valuable time. However, if we take into account the fact that we should avoid overlapping between the observers, the programming process would play a minor role. Finally, a comparative assessment of the fire risk map and the corresponding past burned areas (fire history) will take place in the future in order to evaluate the validity of our model.

5. CONCLUSIONS

The primary objectives of the project have been fulfilled highlighting some crucial conclusions about fire prevention in order to protect the most significant natural resource of the island, namely, the abundant forests. The project incorporated the fire risk modelling in spatial and temporal terms. Specifically, we created a recent comprehensive fire risk map integrating the most contributing natural factors (topography; vegetation conditions and moisture; land cover) and human impacts (proximity to road network and inhabited areas). Afterwards, the most efficient locations for establishing a certain number of watchtowers have been explored in synergy with the previous most recent fire risk map. Finally, the spatiotemporal dimension of fire risk in a time frame of about 20 years has been studied, so that we can detect the influence of the dynamic factors to overall fire risk.

Hence, the most susceptible areas (for 2016) were found on the southwestern and western part of the island as well as in few regions in the north. The cumulative impact of the most affected land cover types (shrubs and forests); the high degree of accessibility and proximity to infrastructures and other artificial structures; the low degree of moisture in some specific areas (especially on the south and northeast part of the study area); and the geomorphological characteristics (low elevation; moderate to steep slope and south aspect) yielded to this specific spatial pattern of fire risk. On the other hand, less affected land cover types with lower degree of accessibility and proximity to artificial structures, higher elevation, north aspect and moderate to higher degree of humidity presented totally different spatial structure. This case is reflected for the broadleaved forests on the north of the island. The same pattern applies to the least affected land cover types (agricultural fields, urban areas) due to the nature of this fuel (quite less flammable), even though other factors may heavily affect the fire risk (accessibility, proximity to inhabited areas; low elevation; south aspect and lower degree of moisture). The fire risk map indicated that 34% of the entire study area is covered by territory of low fire risk; 27% of moderate risk; 34% of high and very high risk, while there is a 6% of the island which is characterized by extremely fire risk.

Similar conclusions with the first fire risk map can be drawn for 1996, since no significant changes have been observed, especially on the land cover types and their spatial arrangement. Again, the spatial arrangement of land covers along with the NDMI index seem to lead and form the fire risk map, since these factors concentrate the highest general weight. The remaining factors indeed affect the fire risk but not as the prevalent force. The fire risk map indicate that 30% of the entire study area is covered by territory of low fire risk; 27% of moderate risk; 36% of high and very high risk, while there is a 7% of the island which is characterized of extremely fire risk.

The spatiotemporal analysis of fire risk highlighted that most of the territory remained within the same fire risk class, followed by decrease of fire risk level and some hotspots with increase of risk levels. These slight changes are due to some specific and certain reasons, such as:

1) Most importantly, the land covers changes. In 2016, more artificial structures have been built, a fact that reduced the fuel for burning. The replacement of forest or agricultural fuel with artificial structures plays a critical role in fire risk; 2) The NDMI index. Even though, the satellite images are derived from the same month (August), it seems that there is much more drought in 1996 compared to 2016 in many territories; 3) Since more artificial structures have been built, a slight increase of fire risk has been occurred due to proximity with these entities. However, the general weight is quite lower than the land cover contribution; 4) The NDVI played a distinct role, since there are very dense and healthy forests in 2016 compared to the high degree of mixture between forests and agricultural fields/shrubs in 1996.

Some good practices to reduce the fire risk especially on the areas where a remarkable (positive) change was noted can include: fuel treatment; recurring monitoring of these susceptible areas for immediate detection of fires through the establishment of watchtowers; utilizing drones and other online platforms with predictive capability of extreme meteorological conditions etc.

Concerning visibility analysis as a supplementary fire prevention measure, we should highlight the fact that there are many cases where higher elevation positions led to very small amount of visibility. So, we should emphasize the impact of geomorphology (slope) that should be taken into account in such projects. In addition, due to this abrupt surface, we saw that the mean visibility potential is only 4%. To this end, we chose the most efficient watchtowers with potential from 8 to 15%.

Specific regions of the study area were adequately covered, while others remained unmonitored. Specifically, the southwestern and the eastern part of the island fall within the visibility potential of multiple watchtowers. The most important fact here is that even though many of the most susceptible areas are not directly visible from the given points, they are located just nearby to the visibility radius of the above positions. Hence, it should be noted that the geomorphology of the study domain plays a prominent role, since most of the watchtowers yielded to marginal visibility range (including the visibility percentages of the examined 31 locations that met the predefined criteria as well as the respective potential of other random points).

Based on the final visibility results, more than 40% of the entire island is visible from the selected location scheme consisting of just 8 watchtowers. The intense topography constituted the most critical barrier in increasing this percentage. In addition, we concluded that almost half of the most risky regions are visible (close to 45%), except the extremely high risk areas where almost 40% is visibly covered. However, this latter category covered only 6% of the study domain.

Finally, it should be highlighted that given the extreme topography of the island, these percentages can be considered satisfying enough, but not optimal. They can be considered satisfying enough in a cost-benefit framework. Otherwise, the establishment of an enormous amount of watchtowers should be demanded, while the added value of each one is quite marginal. This fact includes the demand of very high amount of fiscal resources. Some good practices to counterbalance the relative small

percentage of visibility could include; the extensive patrols in unmonitored regions through the intense road network of the island; the adoption of drones covering the aforementioned areas, especially when extreme meteorological conditions are expected.

BIBLIOGRAPHIC REFERENCES

1) AMALINA, P., PRASETYO, L. B., & RUSHAYATI, S. B. (2016). Forest Fire Vulnerability Mapping in Way Kambas National Park. *Procedia Environmental Sciences*, **33**, 239-252.
2) BAO, S., XIAO, N., LAI, Z., ZHANG, H., & KIM, C. (2015). Optimizing watchtower locations for forest fire monitoring using location models. *Fire Safety Journal*, **71**, 100-109.
3) CARMEL, Y., PAZ, S., JAHASHAN, F., & SHOSHANY, M. (2009). Assessing fire risk using Monte Carlo simulations of fire spread. *Forest Ecology and Management*, **257**(1), 370-377.
4) CASTRO, M., IGLESIAS, L., SÁNCHEZ, J. A., & AMBROSIO, L. (2011). Sight distance analysis of highways using GIS tools. *Transportation research part C: emerging technologies*, **19**(6), 997-1005.
5) CENTER FOR EARTH OBSERVATION, 2017. *How to convert Landsat DNs to Top of Atmosphere (ToA) Reflectance*. [online] Available at: https://yceo.yale.edu/how-convert-landsat-dns-top-atmosphere-toa-reflectance [Accessed 05 Dec. 2017].
6) CHANDER, G., MARKHAM, B. L., & HELDER, D. L. (2009). Summary of current radiometric calibration coefficients for Landsat MSS, TM, ETM+, and EO-1 ALI sensors. *Remote sensing of environment*, **113**(5), 893-903.
7) CHAS-AMIL, M. L., TOUZA, J., & GARCÍA-MARTÍNEZ, E. (2013). Forest fires in the wildland–urban interface: a spatial analysis of forest fragmentation and human impacts. *Applied Geography*, **43**, 127-137.
8) CHEN, Y., YU, J., & KHAN, S. (2010). Spatial sensitivity analysis of multi-criteria weights in GIS-based land suitability evaluation. *Environmental Modelling & Software*, **25**(12), 1582-1591.
9) ENVIRONMENT AND NATURAL RESOURCES (2017). *Government of Northwest Territories Official Website: Environment and Natural Resources: Fire behaviour*. [online] Available at: http://www.enr.gov.nt.ca/programs/fire-operations/fire-behaviour [Accessed 20 Oct. 2017].
10) ERENER, A., MUTLU, A., & DÜZGÜN, H. S. (2016). A comparative study for landslide susceptibility mapping using GIS-based multi-criteria decision analysis (MCDA), logistic regression (LR) and association rule mining (ARM). *Engineering Geology*, **203**, 45-55.
11) EUGENIO, F. C., DOS SANTOS, A. R., FIEDLER, N. C., RIBEIRO, G. A., DA SILVA, A. G., DOS SANTOS, Á. B., ... & SCHETTINO, V. R. (2016). Applying GIS to develop a model for forest fire risk: a case study in Espírito Santo, Brazil. *Journal of Environmental Management*, **173**, 65-71.
12) EUGENIO, F. C., DOS SANTOS, A. R., FIEDLER, N. C., RIBEIRO, G. A., DA SILVA, A. G., JUVANHOL, R. S., ... & PEDRA, B. D. (2016b). GIS applied to location of fires detection towers in domain area of tropical forest. *Science of the Total Environment*, **562**, 542-549.
13) FALCONER, L., HUNTER, D. C., TELFER, T. C., & ROSS, L. G. (2013). Visual, seascape and landscape analysis to support coastal aquaculture site selection. *Land Use Policy*, **34**, 1-10.

14) GABBAN, A., SAN-MIGUEL-AYANZ, J., BARBOSA, P., & LIBERTA, G. (2006). Analysis of NOAA-AVHRR NDVI inter-annual variability for forest fire risk estimation. *International Journal of Remote Sensing*, **27**(8), 1725-1732.

15) GAI, C., WENG, W., & YUAN, H. (2011, April). GIS-based forest fire risk assessment and mapping. In *Computational Sciences and Optimization (CSO), 2011 Fourth International Joint Conference on Computational Sciences and Optimization* (pp. 1240-1244). IEEE.

16) GEOFABRIK (2016). *OpenStreetMap Data Extracts Official Website*. [online] Available at: http://download.geofabrik.de/ [Accessed 23 Nov. 2016].

17) GLOVIS (2017). *USGS Global Visualization Viewer (GloVis)*. [online] Available at: https://glovis.usgs.gov/ [Accessed 10 Oct. 2017].

18) HARIZ, H. A., DÖNMEZ, C. Ç., & SENNAROGLU, B. (2017). Siting of a central healthcare waste incinerator using GIS-Based Multi-Criteria Decision analysis. *Journal of Cleaner Production*, **166**, 1031-1042.

19) HELLENIC STATISTICAL AUTHORITY, 2017. *Hellenic Statistical Authority*. [online] Available at: http://www.statistics.gr/en/home/ [Accessed 3 Oct. 2017].

20) https://landsat.usgs.gov/esun (2017). *Where can I find the solar exoatmospheric spectral irradiances (ESUN) for the Landsat 1-5 MSS, Landsat 4-5 TM, and Landsat 7 ETM+ sensors?* [online] Available at: https://yceo.yale.edu/how-convert-landsat-dns-top-atmosphere-toa-reflectance [Accessed 05 Dec. 2017].

21) JAISWAL, R. K., MUKHERJEE, S., RAJU, K. D., & SAXENA, R. (2002). Forest fire risk zone mapping from satellite imagery and GIS. *International Journal of Applied Earth Observation and Geoinformation*, **4**(1), 1-10.

22) KALABOKIDIS, K., ATHANASIS, N., GAGLIARDI, F., KARAYIANNIS, F., PALAIOLOGOU, P., PARASTATIDIS, S., & VASILAKOS, C. (2013). Virtual Fire: A web-based GIS platform for forest fire control. *Ecological Informatics*, **16**, 62-69.

23) KANT SHARMA, L., KANGA, S., SINGH NATHAWAT, M., SINHA, S., & CHANDRA PANDEY, P. (2012). Fuzzy AHP for forest fire risk modeling. *Disaster Prevention and Management: An International Journal*, **21**(2), 160-171.

24) land.copernicus.eu, 2017. Corine Land Cover - *Copernicus: European Environment Agency*. [online] Available at: http://land.copernicus.eu/pan-european/corine-land-cover [Accessed 11 Oct. 2017].

25) landsat.usgs.gov, 2017. Department of the Interior. U.S. Geological Survey. *Product guide: Landsat surface reflectance-derived Spectral indices*. [online] Available at: https://landsat.usgs.gov/sites/default/files/documents/si_product_guide.pdf [Accessed 21 Oct. 2017].

26) Meteo, 2017a. Meteorological portal – Data derived from National Observatory of Athens. *Station information*. [online] Available at: http://meteosearch.meteo.gr/stationInfo.asp [Accessed 4 Oct. 2017].

27) Meteo, 2017b. Meteorological portal – Data derived from National Observatory of Athens. *Meteorological database*. [online] Available at: http://meteosearch.meteo.gr/default.asp [Accessed 4 Oct. 2017].
28) MITSAKIS, E., STAMOS, I., PAPANIKOLAOU, A., AIFADOPOULOU, G., & KONTOES, H. (2014). Assessment of extreme weather events on transport networks: case study of the 2007 wildfires in Peloponnesus. *Natural hazards*, **72**(1), 87-107.
29) MOUFLIS, G. D., GITAS, I. Z., ILIADOU, S., & MITRI, G. H. (2008). Assessment of the visual impact of marble quarry expansion (1984–2000) on the landscape of Thasos island, NE Greece. *Landscape and urban planning*, **86**(1), 92-102.
30) NCMA, 2017. *National Cadastre and Mapping Agency S.A.* Copyright 2012.
31) NOA, 2017. *National Observatory of Athens*. Diachronic inventory of forest fires. [online] Available at: http://ocean.space.noa.gr/diachronic_bsm/ [Accessed 3 Oct. 2017].
32) NOOROLLAHI, Y., YOUSEFI, H., & MOHAMMADI, M. (2016). Multi-criteria decision support system for wind farm site selection using GIS. *Sustainable Energy Technologies and Assessments*, **13**, 38-50.
33) NURDIANA, A., & RISDIYANTO, I. (2015). Indicator determination of forest and land fires vulnerability using Landsat-5 TM data (case study: Jambi Province). *Procedia Environmental Sciences*, **24**, 141-151.
34) PEREIRA, M. G., ARANHA, J., & AMRAOUI, M. (2014). Land cover fire proneness in Europe. *Forest Systems*, **23**(3), 598-610.
35) POMPA-GARCÍA, M., SOLÍS-MORENO, R., RODRÍGUEZ-TÉLLEZ, E., PINEDO-ÁLVAREZ, A., AVILA-FLORES, D., HERNÁNDEZ-DÍAZ, C., & VELASCO-BAUTISTA, E. (2010). Viewshed analysis for improving the effectiveness of watchtowers, in the north of Mexico. *Open Forest Science Journal*, **3**, 17-22.
36) POMPA-GARCÍA, M., ZAPATA-MOLINA, M., HERNÁNDEZ-DÍAZ, C., & RODRÍGUEZ-TÉLLEZ, E. (2012). Geospatial model as strategy to prevent forest fires: A case study. *Journal of Environmental Protection*, **3**(09), 1034-1038.
37) POURGHASEMI, H. R. (2016). GIS-based forest fire susceptibility mapping in Iran: a comparison between evidential belief function and binary logistic regression models. *Scandinavian journal of forest research*, **31**(1), 80-98.
38) PRADHAN, B., DINI HAIRI BIN SULIMAN, M., & ARSHAD BIN AWANG, M. (2007). Forest fire susceptibility and risk mapping using remote sensing and geographical information systems (GIS). *Disaster Prevention and Management: An International Journal*, **16**(3), 344-352.
39) RIKALOVIC, A., COSIC, I., & LAZAREVIC, D. (2014). GIS based multi-criteria analysis for industrial site selection. *Procedia Engineering*, **69**, 1054-1063.
40) ROBERTO BARBOSA, M., CARLOS SICOLI SEOANE, J., GUIMARAES BURATTO, M., SANTANA DE OLIVEIRA DIAS, L., PAULO CARVALHO RAIVEL, J., & LOBOS MARTINS, F. (2010). Forest Fire Alert System: a Geo Web GIS prioritization model considering

land susceptibility and hotspots–a case study in the Carajás National Forest, Brazilian Amazon. *International Journal of Geographical Information Science*, **24**(6), 873-901.

41) RØD, J. K., & VAN DER MEER, D. (2009). Visibility and dominance analysis: assessing a high-rise building project in Trondheim. *Environment and Planning B: Planning and Design*, **36**(4), 698-710.
42) SAGLAM, B., BILGILI, E., DINCDURMAZ, B., KADIOGULARI, A. I., & KÜÇÜK, Ö. (2008). Spatio-temporal analysis of forest fire risk and danger using LANDSAT imagery. *Sensors*, **8**(6), 3970-3987.
43) SAKELLARIOU, S., TAMPEKIS, S., SAMARA, F., SFOUGARIS, A., & CHRISTOPOULOU, O. (2017). Review of state-of-the-art decision support systems (DSSs) for prevention and suppression of forest fires. *Journal of Forestry Research*, **28**(6), 1107-1117.
44) SAMARA, F. (2016). *Sustainable spatial development model in small islands: The case of Skiathos Island*. PhD Dissertation. Department of Planning & Regional Development, University of Thessaly, Volos, Greece.
45) SÁNCHEZ-LOZANO, J. M., & BERNAL-CONESA, J. A. (2017). Environmental management of Natura 2000 network areas through the combination of Geographic Information Systems (GIS) with Multi-Criteria Decision Making (MCDM) methods. Case study in south-eastern Spain. *Land Use Policy*, **63**, 86-97.
46) SIVRIKAYA, F., SAĞLAM, B., AKAY, A. E., & BOZALI, N. (2014). Evaluation of forest fire risk with GIS. *Polish Journal of Environmental Studies*, **23**(1), 187-194.
47) skiathosisland.com, 2017. *Skiathos island - Geographic data*. [online] Available at: http://skiathosisland.com/skiathos/article/geography [Accessed 03 Oct. 2017].
48) Support.esri.com, 2017a. GIS Dictionary – Slope. [online] Available at: http://support.esri.com/en/other-resources/gis-dictionary/search/slope [Accessed 10 Oct. 2017].
49) Support.esri.com, 2017b. GIS Dictionary – Aspect. [online] Available at: http://support.esri.com/en/other-resources/gis-dictionary/term/aspect [Accessed 10 Oct. 2017].
50) TSAGARI K, KARETSOS G, PROUTSOS N. 2011. *Forest Fires in Greece, 1983-2008*. WWF Hellas and NAGREF-IMFE and FPT (In Greek).
51) USGS, 2017. *NDVI, the Foundation for Remote Sensing Phenology*. [online] Available at: https://phenology.cr.usgs.gov/ndvi_foundation.php [Accessed 21 Oct. 2017].
52) USGS - EARTH EXPLORER, 2017. *Earth Explorer* [online] Available at: https://earthexplorer.usgs.gov/ [Accessed 21 Oct. 2017].
53) VADREVU, K. P., EATURU, A., & BADARINATH, K. (2010). Fire risk evaluation using multicriteria analysis—a case study. *Environmental monitoring and assessment*, **166**(1-4), 223-239.
54) VAN HAAREN, R., & FTHENAKIS, V. (2011). GIS-based wind farm site selection using spatial multi-criteria analysis (SMCA): Evaluating the case for New York State. *Renewable and Sustainable Energy Reviews*, **15**(7), 3332-3340.

55) VILLACRESES, G., GAONA, G., MARTÍNEZ-GÓMEZ, J., & JIJÓN, D. J. (2017). Wind farms suitability location using geographical information system (GIS), based on multi-criteria decision making (MCDM) methods: The case of continental Ecuador. *Renewable Energy*, **109**, 275-286.

56) WIKIPEDIA, 2017. *Skiathos* [online] Available at: https://en.wikipedia.org/wiki/Skiathos [Accessed 3 Oct. 2017].

57) WRÓŻYŃSKI, R., SOJKA, M., & PYSZNY, K. (2016). The application of GIS and 3D graphic software to visual impact assessment of wind turbines. *Renewable Energy*, **96**, 625-635.

58) YALCIN, M., & GUL, F. K. (2017). A GIS-based multi criteria decision analysis approach for exploring geothermal resources: Akarcay basin (Afyonkarahisar). *Geothermics*, **67**, 18-28.

59) YOU, W., LIN, L., WU, L., JI, Z., YU, J. A., ZHU, J., ... & HE, D. (2017). Geographical information system-based forest fire risk assessment integrating national forest inventory data and analysis of its spatiotemporal variability. *Ecological Indicators*, **77**, 176-184.

60) ZHANG, Y. J., LI, A. J., & FUNG, T. (2012). Using GIS and multi-criteria decision analysis for conflict resolution in land use planning. *Procedia Environmental Sciences*, **13**, 2264-2273.

61) ZHOU, D., WANG, B. J., & SHI, B. (2011). GIS viewshed analysis of visual pollution assessment for mine environment. *Guilin Gongxueyuan Xuebao/Journal of Guilin University of Technology*, **31**(2), 207-212.

Masters Program in **Geospatial Technologies**

Supported by:
Education and Culture
ERASMUS MUNDUS